any chemical substance [12]. A highly reactive carbene induced by UV irradiation reacts with CsA, resulting in the production of immobilized CsA in a nonspecific manner. By using the photoaffinity method, we successfully immobilized CsA on resins and performed phage display screening. This method cloned a CsA associated helicase-like protein, which we termed CAHL, and this protein was shown to interact with HCV replication machinery. Our result presents an example for the chemical biological method that could facilitate to reveal a mechanism of viral-cellular interaction.

Results

Phage display screening with immobilized CsA isolated CsA associated helicase-like protein, CAHL

To explore CsA binding proteins, we applied a chemical biology approach. In general, small molecule is necessary to be chemically modified such as biotinylated to be immobilized on solid surface for isolation of binding proteins. However, due to the structural complexity of CsA, it is technically challenging to chemically modify a certain residue of CsA. Therefore, we took advantage of photoaffinity coupling method, which we previously developed [12]. The highly reactive carbene induced by UV irradiation reacted with CsA, resulting in the production of immobilized CsA on solid surface in a nonspecific manner (Fig. 1A). We performed phage display screening with multiple cycles that consist of binding, washing, recovery and amplification (Fig. 1B). We used phage particles randomly displayed 12 amino acids as a library [13]. Through the screening cycles, the ratios of eluted phage particles associated with CsA-immobilized resins comparing to input were dramatically increased (Fig. 1C). We randomly picked up 22 single phage clones from the sixth panning elution (Table S1). Five out of the 22 phage clones were identical, and we called it phage #13. In order to validate the binding specificity of the phage, we amplified phage #13 and measure the ratio of eluted phage titer with CsA and mock resins, which were treated with MeOH to block photoaffinity reaction. The ratio of the phage #13 was 3.75, whereas randomly picked up phage was 1.00. These results indicated that the phage #13 specifically associated with CsA-immobilized resins.

CAHL has an RNA-dependent ATP hydrolysis activity

Phage #13 was predicted to display amino acids, LVFGTLLG-QLRA, in the carboxyl terminus of its phage-coat protein, which is responsible for interaction with CsA. We searched the protein database to find proteins that showed similarities to the LVFGTLLGQLRA sequence. As a result of the search, we found a protein with a sequence identical to LLGQLRA, encoded by a gene accession number NM_022828 in the NCBI database. NM_022828 is predicted to encodes 1430 amino acid protein that has a couple of conserved domains, such as DEXHc helicase, RNA-dependent ATPase and ankyrin repeat (Fig. 2A; Fig S1). LLGQLRA sequence is located in the middle region of the protein (amino acids 940–946), where is no known conserved motif is found (Fig. 2A). Since it has not been reported on its biological functions, hereafter we refer to the NM_022828 as CsA-associated helicase-like protein, CAHL. To confirm the interaction between CAHL and CsA, we prepared a recombinant C-terminal protein of CAHL (named CAHL-C) that consisted of amino acids 761 to 1430 (Fig. 2B) including LLGQLRA motif, and performed surface plasmon resonance (SPR) analysis. It was difficult to use a full-length CAHL for *in vitro* pull-down assays since obtaining enough amount of full-length CAHL for SPR was technically challenging due to high insolubility. Considering that CsA binding sequence

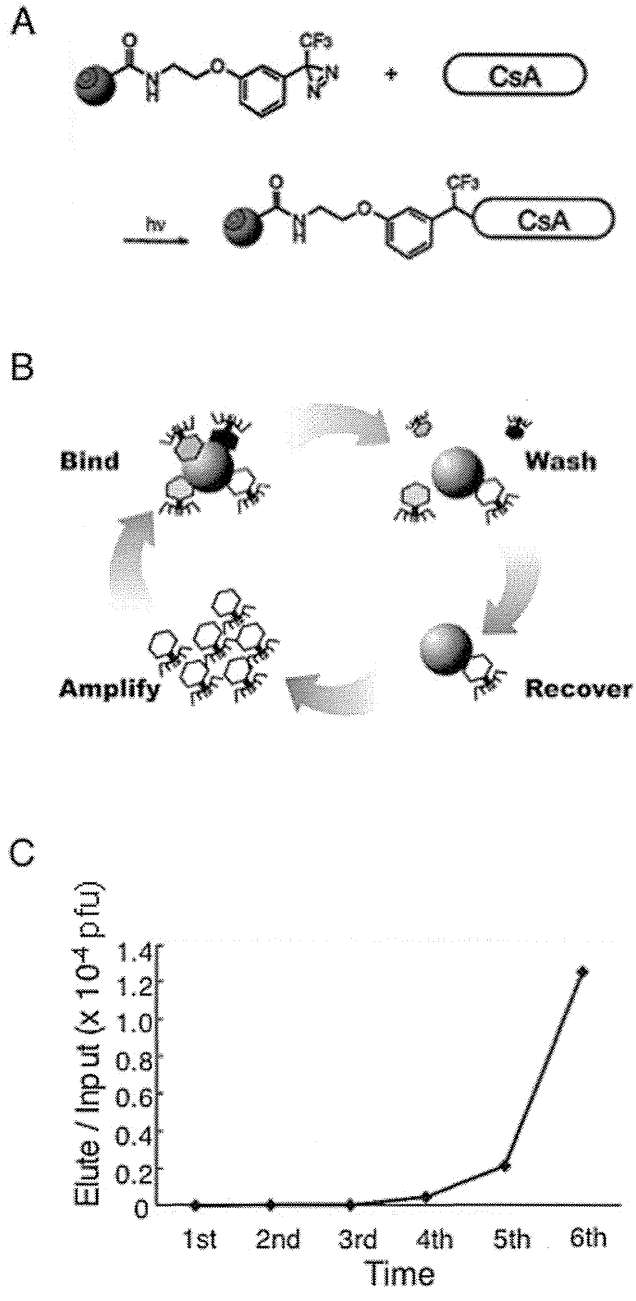

Figure 1. Immobilization of CsA and phage display screening. (A) A schematic diagram of CsA immobilization on photoaffinity resins. (B) Procedure of phage display screening. (C) Relative enrichment of phage particles. Relative enrichment was determined by the relationship between phage titer of elution from a CsA immobilized resins and input.
doi:10.1371/journal.pone.0018285.g001

found by the phage display screening is located C-terminus of CAHL, we used CAHL-C protein. A specific binding response with CsA was observed ($KD = 1.2 \times 10^{-7}$ M), whereas those with FK506, which is an immunosuppressant and has no HCV-inhibitory activity, were significantly weak ($KD = 2.5 \times 10^{-6}$ M) (Fig. 2C). Since CAHL was predicted to be RNA-dependent ATPase based on conserved domains (Fig. 2A), we measured the ATPase activity of CAHL in the presence and absence of RNA. As shown in Fig.2D, RNA-dependent ATP hydrolytic activity of CAHL-C was clearly observed, and this activity was suppressed in

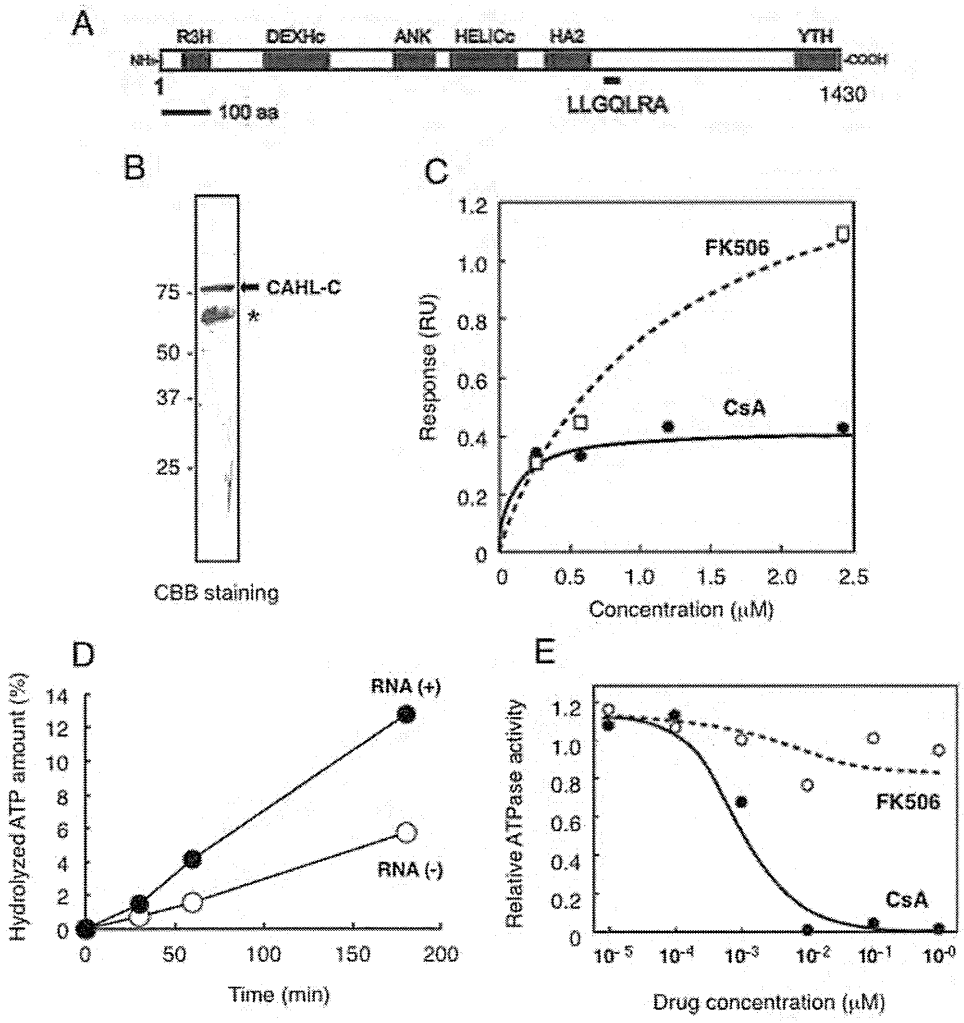

Figure 2. Cloning of CsA associated helicase-like protein (CAHL) by phage display screening. (A) Schematic representation of CAHL protein. R3H (*cd*02325), DEXHc (*cd*00269), ANK (*cd*00204), HELICc (*smart*00490), HA2 (*pfam*04408) and YTH (*pfam*04146) motifs were found by a CD search (http://www.ncbi.nlm.nih.gov/Structure/edd/wrpsb.cgi). Underline indicates a region of the LLGQRA amino acid sequence identical to the CsA-associated sequence displayed on phage #13. (B) Purified recombinant CAHL-C protein was confirmed by SDS-PAGE analysis (arrow). Asterisk indicates degraded products. (C) A kinetic plot and binding isotherm for binding of CsA (closed circle) and FK506 (opened square) to CAHL-C sensor chips in concentrations ranging from 0.25 to 2.5 mM. The estimated KD value of interaction between CAHL-C and CsA or FK506 was 1.2×10^{-7} or 2.5×10^{-6} M, respectively. (D) RNA-dependent ATP hydrolytic activities of CAHL. Filled and open circles indicate ATP hydrolytic activities of CAHL in the presence (closed circle) or absence (opened circle) of total RNA extracted from liver cells, respectively. (E) CsA inhibitory effects on ATP hydrolytic activities of CAHL. Filled and open circles indicate ATP hydrolytic activities with CsA (closed circle) or FK506 (opened circle), respectively.
doi:10.1371/journal.pone.0018285.g002

a dose-dependent manner when CsA, but not FK506 (Fig. 2E). A difference of inhibitory effects of CsA and FK506 on CAHL-C hydrolytic activity is more than 2-orders of magnitude. Considering that the difference of *KD*s of CsA and FK506 values measured by SPR, CsA association with CAHL would significantly affect on the activity. These results indicate that CAHL had RNA-dependent ATPase activity and was specifically inhibited by CsA.

CAHL is localized in ER and its expression is up-regulated by TNF-α treatment

Since biological functions of CAHL were unknown, we investigated the biological background of the CAHL gene. We first performed RNA blotting analysis and RT-PCR using normal human tissues and tumor cells. As shown in Fig. 3A, CAHL-transcripts with approximately 1.6 kbp were detected in both human hepatoma Huh-7 cells and MH-14 cells, which do not and do carry the HCV subgenome replicon, respectively, whereas much less was detected in normal liver tissues. RT-PCR analysis revealed that in other normal tissues (though not testis) little or no expression of CAHL was observed as compared the house-keeping gene G6PDH, whereas clear expression of it was detected in all the tumor cell lines examined (Fig. 3B). Since the CAHL expression was very little in the normal liver tissues, a question was arisen: how is CAHL expression regulated? It is possible that CAHL could be induced by inflammation caused by virus infections. To test the hypothesis, we observed whether CAHL expressions are induced by inflammatory signals. Indeed, CAHL in normal liver cells was upregulated in the presence of a proinflammatory cytokine, tumor necrosis factor (TNF)-α with dose dependent manner (Fig. 3C), suggesting that CAHL can express to some extent in the liver under chronic hepatitis. Next, we observed CAHL subcellular localization in Huh-7 and MH-14 cells using an anti-CAHL antibody (Fig. 3D). Fluorescence derived from CAHL

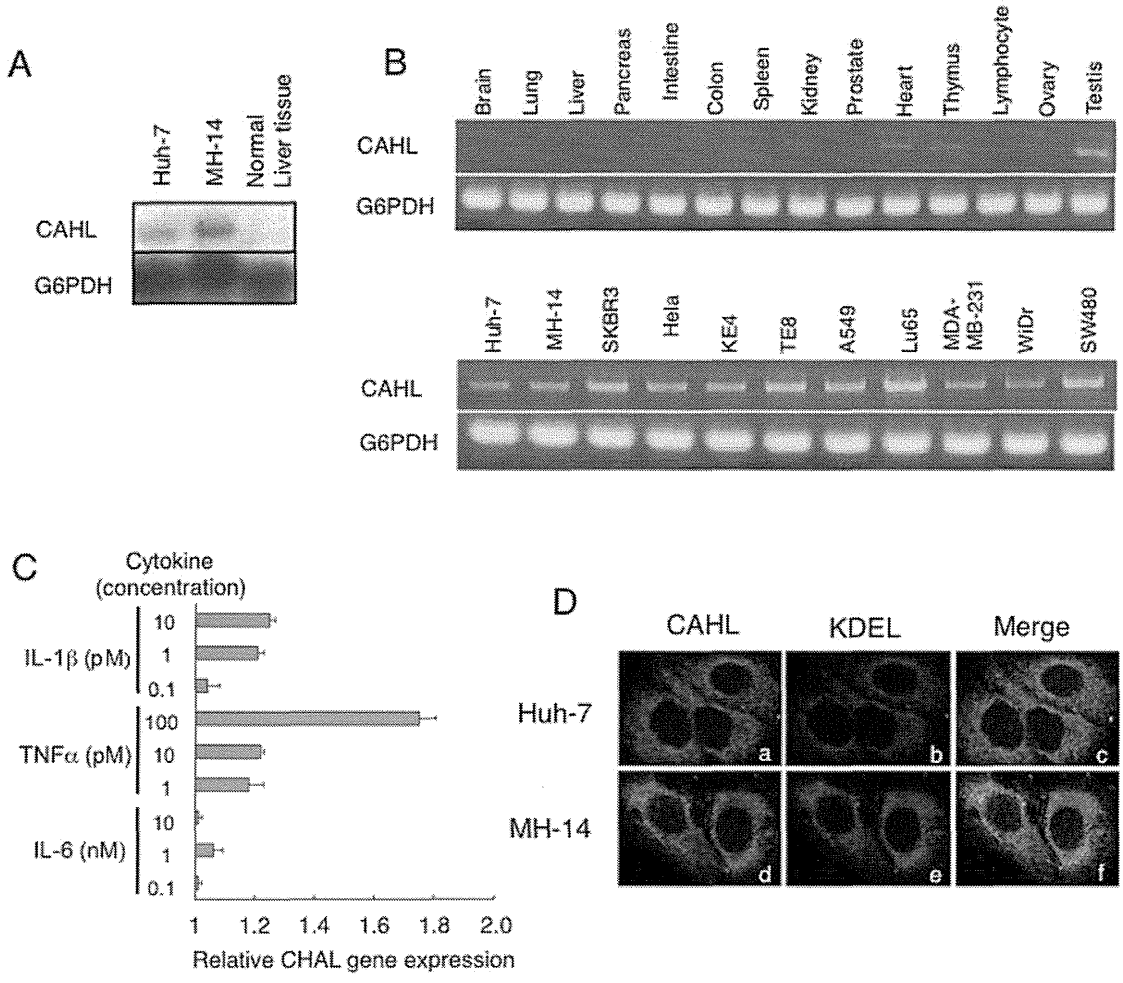

Figure 3. Expression profile of CAHL. (A) For Northern blot analysis, CAHL and G6PDH as an internal control were detected in RNAs derived from Huh-7 and MH-14 cells, as well as normal liver tissues. (B) RT-PCR analysis for CAHL, and G6PDH as an internal control, were performed using RNAs derived from normal human tissues and tumor cells. (C) CAHL in normal liver cells was upregulated by TNF-α. Normal liver cells were cultured in the presence of proinflammatory cytokines, IL-1β, TNF-α, and IL-6 at the indicated concentrations for 8 h. Subsequently, cells were harvested, and measurement of these cells derived-CAHL gene expression by quantitative analysis by was performed using the LightCycler system. These data represent as relative rates (1 = non-treated cells). Error bars represent the standard error of the mean. (D) Colocalization of CAHL with KDEL as an endoplasmic reticulum (ER) marker. Indirect immunofluorescence analysis was performed on Huh-7 and MH-14 cells. Cells stained with anti-CAHL (panels a and d, green) and an anti-KDEL mAb (panels b and e, red) for ER identification as a marker used as a primary antibody followed by Alexa Fluor 488-conjugated goat anti-rabbit and 594-conjugated goat anti-mouse antibodies, respectively. Merged images of green and red signals are shown in panels c and f.The optically merged image is representative of most cells examined by laser confocal microscopy. Original magnification: x1000.
doi:10.1371/journal.pone.0018285.g003

demonstrated that CAHL was co-localized with KDEL protein as a marker for endoplasmic reticulum (ER) in both the presence (MH-14 cells) and absence (Huh-7 cells) of the HCV subgenome, indicating that CAHL could localize in ER with HCV independent manner. Moreover, it was observed that CAHL also colocalized with HCV-derived proteins such as NS3, NS4A, NS4B, NS5A and NS5B localized in ER (Fig. S2). Thus, these data strongly suggested that CAHL would localize in ER.

Association of CAHL, NS5B and CyPB

Since CAHL interacts CsA, which has inhibitory effects to HCV replication, it is interesting to investigate the molecular interactions of CAHL and HCV-derived molecules involving the replication machinery. Intriguingly, the purified full-length CAHL fused to GST was coprecipitated with NS5B but not NS3, NS4B or NS5A protein, as shown in Fig. 4A. To determine a regions of NS5B responsible for binding with CAHL, various dissected NS5B proteins were subjected to pull-down assays, resulting in that two separated regions (1–200 aa or 401–520 aa) of NS5B were sufficient for the interaction with CAHL (Fig. 4B). In addition to the CAHL and NS5B interaction, we found interaction between CAHL and CyPB, but not CyPA (Fig. 4C). The interaction of CAHL and CyPB was disrupted with presence of CsA, whereas the association of CAHL with NS5B was not (Fig. 4D). These results suggest that trimer complex consisting of CAHL, CyPB and NS5B could form.

CAHL has a main role in HCV-replication via NS5B

The finding that CAHL structurally associated with the CyPB/NS5B complex in cell-free assessment prompted us to examine whether this trimer complex could act for HCV genome replication *in vivo*. First, five small interference RNAs (siRNA)

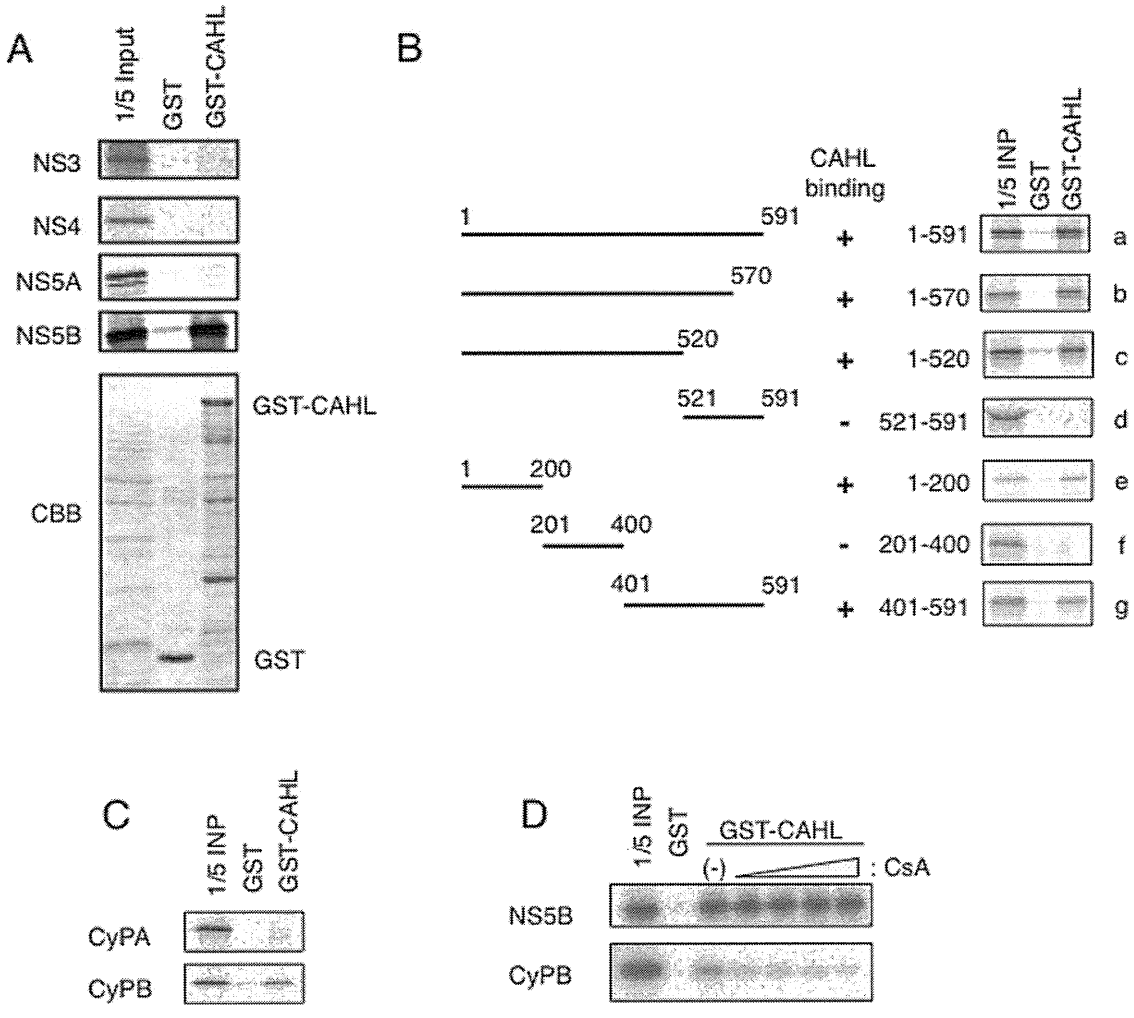

Figure 4. CAHL interacted with HCV NS5B and CyPB. (A) [^{35}S]-labeled in vitro translation products of HCV NS3, NS4B, NS5A, and NS5B were incubated with a recombinant GST fusion protein of CAHL (GST-CAHL) or GST as a negative control. "1/5 input" designates the signal for 1/5 the amount of the [^{35}S]-labeled product used in the pull-down assay. CBB staining patterns for the pulled-down proteins are shown in the bottom panel. (B) Mapping of the regions of NS5B responsible for the interaction with CAHL. At the left of the panel, schematic representations of the full-length and truncated mutants of NS5B are shown. The numbers indicate the amino acid residue numbers in NS5B. "CAHL binding" summarizes the results of the GST pull-down assay by +/−. GST pull-down data are presented as described in (A). (C) GST pull-down assay between GST-CAHL and in vitro translated CyPA or CyPB was performed as described in (A). (D) The interaction of CAHL with CyPB was disrupted by CsA treatment. GST pull-down assay between GST-CAHL and NS5B was performed in the absence and presence of CsA. The concentrations of CsA in lanes 4–7 are 1, 2, 8, and 20 μg/ml, respectively.
doi:10.1371/journal.pone.0018285.g004

specific for the CAHL gene (si-1, -2, -3, -4, and -5) were individually transfected into MH-14 cells to examine RNA sequence induced effectively down-regulation. When si-3 siRNA was transfected into cells, the endogenous CAHL gene expression reduced approximately 90% compared with si-control (treatment with siRNA for non-target gene) (Fig. S3), and among them, si-3 induced down-regulation of CAHL gene expression most effectively. Subsequently, we applied short hairpin RNA (shRNA) technology to stably knockdown CAHL gene expression in MH14 cells. We cloned DNA oligo coding the effective siRNA against CAHL gene into pLKO.1-puro shRNA vector. Lentivirus packed with shRNA against CAHL (sh-CAHL) or non-targeting shRNA (sh-control) were introduced into MH14 cells, and then these cells were cultured in the presence puromycin. As a result, we successfully obtained stably CAHL gene knockdown cell line, which reduced approximately to 6-fold compared with sh-control (Fig. 5A). In these sh-CAHL cells, HCV RNA was decreased approximately to 4-fold less than that in the sh-control cells (Fig. 5B). Furthermore, ectopic expression of CAHL increased the HCV replication level in a dose-dependent manner (Fig. 5C). These results suggest that CAHL positively plays in HCV replication.

To investigate the outcome of the interaction of CAHL with NS5B/CyPB, we performed RNA binding activity assay using sh-CAHL cells. NS5B is a viral RNA-dependent RNA polymerase and possesses RNA binding activity [11]. Indeed, NS5B formed a complex on RNA-immobilized sepharose together with CyPB and CAHL (lane 4 in Fig. 6A). However, shRNA-mediated depletion of endogenous CAHL dissociated CyPB from the NS5B/RNA complex (lane 6 in Fig. 6A), indicating that CAHL mediates the association of CyPB with NS5B/RNA. Moreover, when CsA was added to sh-CAHL cells, both CAHL and CyPB were dissociated from RNA (lane 6 in Fig. 6B). Thus, the possibility is suggested that the promotion of CyPB-NS5B complex association by CAHL is related with the stimulatory role of CAHL in HCV replication.

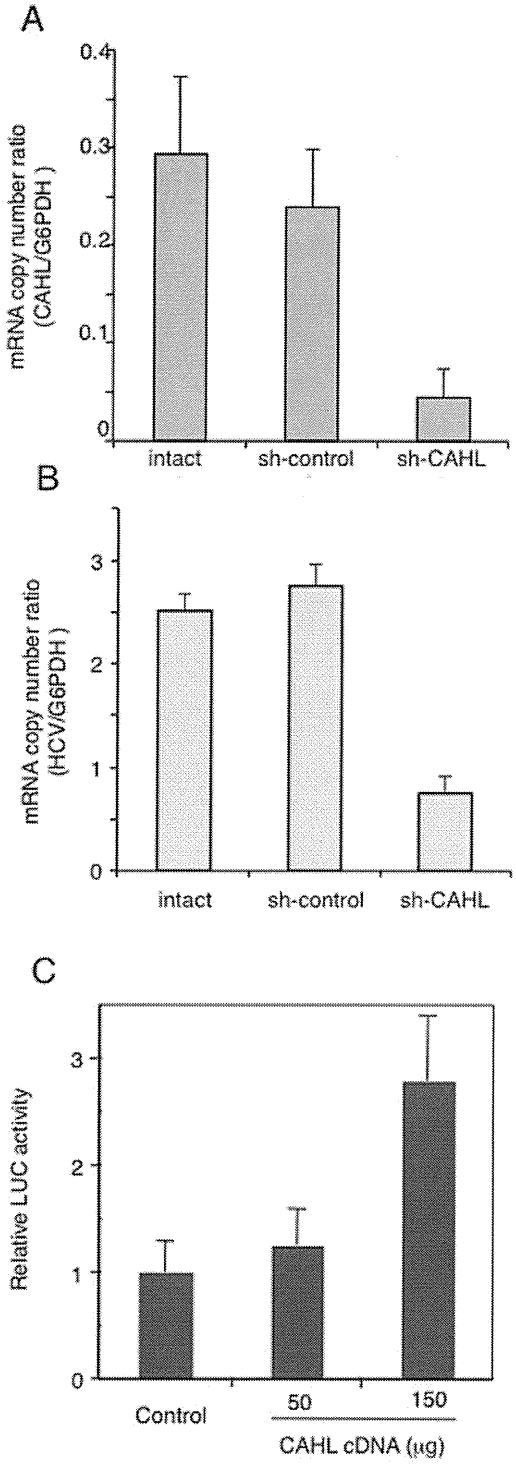

Figure 5. Establishment stably CAHL knockdown cell. (A) Lentivirus packed with shRNA against CAHL (sh-CAHL) or non-targeting shRNA (sh-control) were introduced into MH14 cells. Total RNAs were harvested and the absolute mRNA copy numbers of CAHL were examined by quantitative real time RT-PCR. (B) The same samples of total RNAs were used for the measurement of the absolute RNA copy number of the HCV genome by quantitative real time RT-PCR. (C) Cured MH-14 cells were transfected with LMH14 RNA reporter together with the expression plasmid for CAHL or the corresponding empty vector. At four days post-transfection, luciferase activities were measured. These results (A–C) represent the means of three independent experiments.
doi:10.1371/journal.pone.0018285.g005

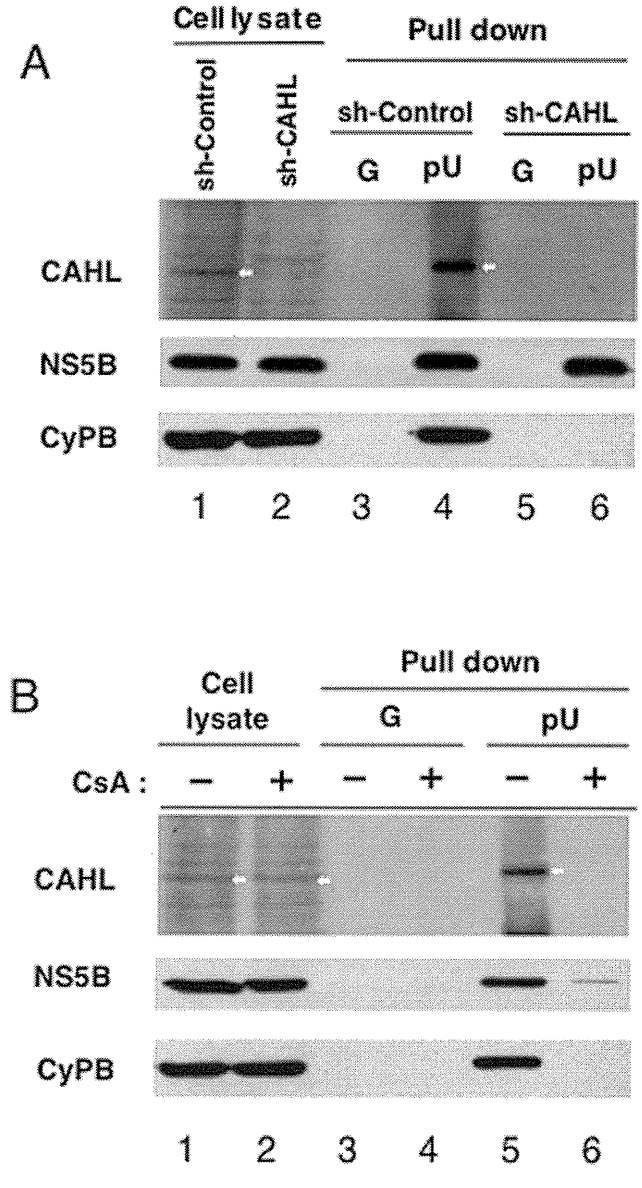

Figure 6. CAHL associated with the CyPB/NS5B complex plays critical roles in HCV replication. (A) Cells (sh-control or sh-CAHL cells) were harvested and analyzed protein expressions by using anti-CAHL, anti-NS5B, and anti-CyPB antibodies. White arrows indicate CAHL protein. (B) Cells were treated with or without 2 μg/ml CsA for 24 h, and then harvested and analyzed. These results were reproduced in three independent experiments. White arrows indicate CAHL protein.
doi:10.1371/journal.pone.0018285.g006

Discussion

Phage display, invented by Smith and Petrenko, is a versatile method for the detection of small molecule-binding proteins [14]. The technique can also be used to identify binding sites within the target protein itself. The combination of screening a library of phage-displayed peptides and analysis of affinity-selected peptides is anticipated to become a powerful tool for identifying drug-binding sites [15–19]. Screening phage display libraries generally entails immobilizing the drug onto a solid surface [20]. In the conventional method of phage display, small molecules should be converted into biotinylated derivatives and immobilized on a streptavidin-coated matrix. Conventional immobilization requires

the presence of desirable functional groups within the drug molecule as well as a multistep process to prepare the biotinylated derivatives. In contrast to biotinylation, photoimmobilization makes it possible to covalently immobilize drugs on a solid surface without the need for derivatization. We and Kanoh *et al.* have reported the affinity purification of proteins using affinity matrices, in which small molecules are photoimmobilized by photoreaction [12,21]. Because the photoreaction proceeds in a functional group-independent manner, the molecules are immobilized onto the solid surface in a nonoriented fashion. Thus, photoimmobilization can be a useful tool for the comprehensive analysis of drug-binding proteins.

Using this method, we identified CAHL as a novel target protein for CsA. CsA is a natural compound showing multiple biological activities, including an immunosuppressive function, anti-chaperone activity, inhibition of transporter activity and anti-viral activity against human immunodeficiency virus and HCV. Thus far, p-glycoprotein and formyl peptide receptor, as well as CyPs, were reported as binding proteins for CsA [22], which enabled elucidation of the mechanism of the CsA-induced immunosuppressive function, anti-chaperone activity and anti-transporter activity, respectively. Although CyPA promotes HCV replication [11,23,24], we cannot fully explain the whole mode of action of CsA against HCV. CyPB is also reported to regulate HCV replication. It was reported that the HCV replicon showing resistance against the CsA-mediated anti-HCV effect possessed mutations in the coding region for NS5A and NS5B [25,26], indicating that NS5B was one of the determinants for the sensitivity to CsA. However, some such mutations within the NS5B coding region were dropped outside the region interacting with CyPA and CyPB [11,24], leading to the possibility that another cellular protein which is targeted by CsA, binds to NS5B and regulates HCV replication. The CAHL-NS5B regulation machinery is consistent with this idea. Deletion analysis for NS5B demonstrated that two separate regions (1-200aa and 401-520aa) of NS5B are likely to be involved in the interaction with CAHL. These regions are different from the NS5B domain interacting with CyPB (521-591aa) [11], suggesting that NS5B would interact with both CyPB and CAHL at the same time. Indeed, the mutations that induced resistant to CsA, the I432V in NS5B reside inside the regions interacting with CAHL (1-200 aa and 401-520 aa) [26], supported the relevance of CAHL in HCV genome replication. As another aspect, it is interesting that two CsA target molecules interact with each other and NS5B. Although we do not know in detail the implication of the interaction of these two CsA target molecules, CyPB and CAHL, there is a similar example already known: two FK506-binding proteins, P-glycoprotein (P-gp) and FKBP42, associate with each other [27]. In this situation, FKBP42 modulates P-gp function. We do not know in detail how these two target molecules of CsA, CyPB and CAHL both regulate NS5B function, which is a future subject of the study. Currently, a CsA derivative shows remarkable anti-HCV effect in chronic HCV-infected patients in the phase II clinical trial, and its mode of action needs to be fully clarified [28]. Our data suggest a new link of CAHL, in addition to CyP family, with CsA derivative's anti-HCV activity.

Cellular RNA helicases have been reported to be involved in HCV genome replication. DDX3 and DDX6 activate HCV genome replication through yet unknown mechanism [29,30]. RNA helicase p68 (DDX5) interacts with NS5B and supports HCV genome replication in a transient transfection assay [31]. Although the mechanism through which each RNA helicase regulates HCV genome replication may be different, the requirement of cellular RNA helicases for HCV genome replication is interesting for understanding HCV-cellular factors interaction.

CAHL expression in normal liver cells was much less than that in HCV infectious cells such as Huh-7 and MH-14. This is enigmatic since it is not clear how HCV replication start without CAHL, which positively plays HCV replication, at very beginning of HCV infection in normal liver cells. It was reported that a proinflammatory cytokine, TNF-α gene expression in hepatocytes and mononuclear cells derived from HCV carrier increased compared with healthy control [32]. As we here demonstrated CAHL induced by TNF-α, CAHL can express to some extent in the liver under chronic hepatitis C. We also show the association of CAHL with HCV replication. Taken together, CAHL may form a positive feedback loop for HCV replication: CAHL gene expression is induced by TNF-α that is highly upregulated by HCV infection, and CAHL in turn promotes HCV replication. Despite the low expression of CAHL in normal tissues, CAHL may have strong potential as a pharmaceutical target protein. In addition to CsA, isolation of specific inhibitors to the interaction of CAHL and NS5B could allow us to provide effective drug for HCV treatment.

In conclusion, we took advantage of strategy of chemical biology to isolate a cellular factor, CAHL, as CsA associated helicase-like protein, which would form trimer complex with CyPB and NS5B of HCV. These findings not only shed a light on new HCV treatment but also brought about great values of chemical biology to elucidate biological mechanisms of small-molecule and protein interactions.

Materials and Methods

Preparation of CsA-immobilized resins

CsA was purchased from Wako Pure Chemical Industries, Ltd. (Osaka, Japan). CsA-immobilized resins were prepared on photoaffinity resins as described previously [12]. Photoaffinity resins treated with UV irradiation in the absence of CsA were used for negative control.

Phage display screening

10 mg of CsA-immobilized resin was incubated in 1 ml of TBS (50 μM Tris-HCl [pH 8.0] and 150 mM NaCl) for 12 hours or longer before use. Phage screening conditions were performed as previously described [20]. For each panning step, 50 μl of CsA-immobilized resin slurry was added to 1 ml of the T7 phage ($>10^{11}$ pfu) followed by incubation for 8 hours at 4°C. After incubation, the bead slurry was washed 10 times by adding 1 ml of TBST (50 mM Tris-HCl [pH = 8.0], 150 mM NaCl, 0.1% Tween 20). To elute phage particles associated with resins, 100 μl of *Escherichia coli* ($OD_{600} = 0.6$) was added, and incubated for 10 min at 37°C. The phage infected *E. coli* were transferred into 1 ml of *E. coli* ($OD_{600} = 0.6$) and grown until lysed for three hours at 37°C with shaking. For titer check, 10 μl of infected *E. coli* was used.

RNA preparation and plasmid construction

To isolate the CAHL gene, we used total RNA derived from human liver. DNA cloning of the CAHL gene was carried out using a SMART-cDNA isolation kit following the manufacturer's instructions (Clontech Laboratories, CA, USA). In some cases, CAHL cDNA was reconstructed with pcDNA 3.1 myc-HisA (Invitrogen Corp., CA, USA) for overexpression experiments.

Surface plasmon resonance assay

SPR analysis was performed on a BIAcore 3000 (Biacore AB, Uppsala, Sweden). The bacterially expressed CAHL-C was

immobilized covalently on a hydrophilic carboxymethylated dextran matrix on a CM5 sensor chip (Biacore AB) using a standard amine coupling reaction in 10 mM CH_3COONa [pH = 4.0]. Binding analyses were carried out in HBS-EP buffer (10 mM HEPES [pH = 7.4], 150 mM NaCl, 3.4 mM EDTA, 0.005% surfactant P20) containing 8% DMSO at a flow rate of 20 µl/min. Appropriate concentrations of CsA were injected over the flow cell. CyPA or CyPB was not used as a positive control because of two reasons: 1) those CyPs can be used for a positive control as CsA-CyP binding, but not for CsA-CAHL binding, and 2) FK506 doesn't bind CyPs, so that it is difficult to compare association behaviors between FK506 and CsA. The bulk effects of DMSO were subtracted using reference surfaces. To derive binding constants, data were analyzed by means of global fitting using BIAevaluation version 3.1 (Biacore AB).

Preparation of recombinant protein

CAHL-C cDNA encoding C-terminal 761 to1430 amino acids was constructed into pET21a prokaryotic expression vector (Merck, Darmstadt, Germany), which has a His-tag. pET21-CAHL-C construct was transformed into *E.coli* BL21(DE3) strain. After overnight induction with 0.1 mM IPTG at 20°C, recombinant CAHL-C was purified by nickel column chromatography with HisTrap (Amersham biosciences, Uppsala, Sweden) according to a manufacturer's procedure. To concentrate and exchange the buffer, purified CAHL-C was concentrated up to 40 times with PBS by using Amicon Ultra 30 (Millipore, EMD, Germany).

ATPase assay

ATPase activity was measured as described by Okanami *et al.* [33]. Briefly, CAHL-C protein (500 ng) was incubated in 50 µl of helicase/ATPase buffer containing 1 µl of [γ-^{32}P]ATP (1 Ci/µmol) in the presence or absence of 100 ng of total RNA derived from liver at 30°C for 30, 60, and 180 min. An aliquot (10 µl) was removed at the appropriate time and added to 200 ml of a solution containing 50 mM HCl, 5 mM H_3PO_4 and 7% activated charcoal. After the charcoal was precipitated by centrifugation to remove unreacted ATP, 10 µl of the supernatant was subjected to Cerencov counting to quantitate released [^{32}P]phosphate.

Northern blot analysis and reverse transcription PCR (RT-PCR) analysis

Tumor cell-derived total RNA was prepared using an RNeasy Mini Kit (QIAGEN Inc., Hilden, Germany) according to the manufacturer's instructions and then reverse-transcribed to cDNA with Transcriptor First Strand cDNA Synthesis Kit (Roche Applied Science, Mnnheim, Germany). A reverse-transcribed single strand DNA library of normal tissues was purchased from Clontec, Inc. (CA, USA). In Northern blot analysis, RNA samples were loaded to formaldehyde agarose gels and transferred onto a Hybond N membrane (GE Healthcare UK Ltd., Buckinghamshire, England). After UV-crosslinking, the membrane was hybridized with ^{32}P-labeled (Rediprime II, GE Healthcare) gene-specific probe, regions of $CAHL_{2913\text{-}4431}$ and human $G6PDH_{454\text{-}2016}$ and exposed to film for autoradiography. Measurement of CAHL gene expression by polymerase chain reaction (PCR) was performed using GoTaq Flexi DNA Polymerase (Promega, Co. WI, U.S.A.) and primer sets: forward primer, 5′-GACGGGAAAGGATTGGTCAA-3′ and reverse primer, 5′-CATCACTTCGTGCTTTTT-3′ for detection of CAHL, and forward primer, 5′-GACGAAGCGCAGACAGCGTCATGGCA-3′ and reverse primer, 5′-GCTTGTGGGGGTTCACCCACTTG-3′ for detection of G6PDH.

Quantitative real-time RT-PCR analysis

Total RNAs reverse-transcribed to cDNA were prepared as described above. Measurement of gene expression by quantitative analysis was performed using the LightCycler system (Roche Applied Science). Primers and hybridization probes were synthesized by Nihon Gene Research Laboratory Inc. (Sendai, Japan). Quantitative real time RT-PCR analyses of human glucose-6-phosphate dehydrogenase (G6PDH) and cyclosporin A associated helicase-like protein (CAHL, NM_022828) gene expression were performed using the LightCycler® FastStart DNA MasterPLUS SYBR Green I system (Roche Applied Science) with the following primer sets: forward primer, 5′-CTGCGTTATCCTCACCTTC-3′ and reverse primer, 5′-CGGACGTCATCTGAGTTG-3′ for detection of human G6PDH; forward primer, 5′-GTGT-CTGGACCCCATCCTTA-3′and reverse primer, 5′-CCCAT-CACTTCGTGCTTTTT-3′for detection of CAHL. Gene expression analysis of the HCV genome was performed using the LightCycler® FastStart DNA Master HybProbe system (Roche Applied Science) with the following primer set and probe: forward primer, 5′-CGGGAGAGCCATAGTGG-3′ and reverse primer, 5′-AGTACCACAAGGCCTTTCG-3′, and the fluorogenic probe, 5′-CTGCGGAACCGGTGAGTACAC-3′. PCR amplification of the housekeeping gene, G6PDH, was performed for each sample as control for sample loading and to allow normalization among samples. To determine the absolute copy number of the target transcripts, the fragments of G6PDH or target genes amplified by PCR using the above described primer set were constructed with pCR4®-TOPO® cloning vector (Invitrogen). The concentrations of these purified plasmids were measured by absorbance at 260 nm and copy numbers were calculated from concentration of samples. A standard curve was created by plotting the threshold cycle (Ct) versus the known copy number for each plasmid template in the dilutions. The copy numbers for all unknown samples were determined according to the standard curve using LightCycler version 3.5.3 (Roche Applied Science). To correct for differences in both RNA quality and quantity between samples, each target gene was first normalized by dividing the copy number of the target by the copy number of G6PDH, so that the mRNA copy number of the target was the copy number per the copy number of G6PDH. The initial value was also corrected for the amount of G6PDH indicated as 100% to evaluate the sequential alteration of the mRNA expression level.

Cell culture and transfection of siRNA and cDNA

The human tumor cell lines of breast adenocarcinoma MDA-MB-231, lung adenocarcinoma A-549, colon adenocarcinoma WiDr, hepatocellular carcinoma Huh-7, breast cancer SKBR3, cervical carcinoma HeLa, esophagus cancer KE-4, colon adenocarcinoma SW480, lung cancer Lu65, and esophagus squamous cell carcinoma TE-8 were obtained from Health Science Research Resources Bank (Sendai, Japan). These cells were cultured in Dulbecco's modified Eagle's medium (Huh-7, SKBR3, HeLa, KE-4, and SW480 cells), RPMI 1640 (A-549, WiDr, TE-8, and Lu65 cells) (SIGMA-ALDRICH, MO, USA), and Leibovitz's L15 (MDA-MB-231 cells) (Invitrogen) supplemented with 10% fetal bovine serum, MEM nonessential amino acids (Invitrogen), 200 unit/ml penicillin (Invitrogen), 200 µg/ml streptomycin (Invitrogen) and 2 mM L-glutamine (Invitrogen). MH-14 cells carrying the HCV subgenomic replicon [34] were cultured in the DMEM medium supplemented with 10% fetal bovine serum, MEM nonessential amino acids (Invitrogen), 200 unit/ml penicillin (Invitrogen), 200 µg/ml streptomycin (Invitrogen), 2 mM L-glutamine (Invitrogen) and 300 µg/ml G418 (Invitrogen). Five small interfering RNA (siRNA) duplexes containing 3′dTdT over

the hanging sequence were synthesized (Sigma-Aldrich, St. Louis, MO). These sequences were: si-1; 5′-GGACAUUCGCAUUGAUGAG-3′, si-2; 5′-CCUGUAAUUUGACUCAUAA-3′, si-3; 5′- GCCUUGGAUGUAAAUCUCUUU -3′, si-4; 5′- GGAGCUUUCAGUGACCAUA -3′, si-5; 5′-GGUCAAAUAAUAGUAGGAA-3′. A non-targeting siRNA (Sigma-Aldrich) was used as control. Plasmid and siRNA transfection was performed described previously [35]. In siRNA study, total RNAs from transfected cells were harvested after transfection for 5 days and examined mRNA copy number of CAHL by quantitative real-time RT-PCR.

Establishment of stable CAHL-knockdown cell by shRNA

Based on the siRNA data, we applied short hairpin RNA (shRNA) technology platform (Sigma Mission*RNAi*) to stably knockdown CAHL gene expression in MH14 cells. DNA oligo coding the effective siRNAs against each MH14-CAHL gene (5′-CCGGGCCTTGGATGTAAATCTCTTTCTCGAGAAAGAGATTTACATCCAAGGCTTTTTTG -3′) (sh-CAHL) was cloned into pLKO.1-puro shRNA vector. Plasmid DNA including non-targeting shRNA as control (sh-control) was transfected into MH14 cells along with Lentiviral Packaging Mix consisting of an envelope and packaging vector (Sigma-Aldrich) to produce lentivirus packed with shRNA cassettes using the standard procedure. After transfection, cells were cultured in the presence of 10 μg/ml puromycin.

Indirect immunofluorescence analysis

Anti-CAHL polyclonal antibody serum was generated in rabbits immunized with $CAHL_{1237\text{-}1251}$, ILHPKRGTEDRSDQS, according to our lab protocol [35]. Anti-NS3, NS4B, and NS5B, and NS5A were kindly provided from Dr. Kohara at The Tokyo Metropolitan Institute of Medical Science, Japan and Dr. Takamizawa at Osaka University, Japan, respectively. Cells were fixed with ice-cold acetone for 1 min, and then stained with anti-CAHL and anti-KDEL mAb (Santa Cruz Biotechnology, CA, USA) for ER antibodies followed by Alexa Fluor 488-conjugated goat anti-rabbit IgG and 594-conjugated goat anti-mouse IgG (Invitrogen), respectively, and visualized using a Bio-Rad MRC1024ES laser confocal scanning microscopy system (Bio-Rad Laboratories, CA, USA).

Immunoblot analysis

Immunoblot analysis was performed essentially as described previously [11,36].

RNA-protein binding precipitation assay

RNA-protein binding precipitation assay was essentially performed as described [11]. Briefly, to permeabilize plasma membrane, cells were treated 50 μg/ml digitonin (Nakarai Tesque Inc., Kyoto, Japan) in buffer B (20 mM HEPES-KOH [pH = 7.7], 110 mM KOAc, 2 mM MgOAc, 1 mM EGTA) at 25°C for 5 min. After treatment with 0.5 μg/ml proteinase K at 37°C for 5 min and washing with buffer B, cells were lysed in IP buffer (50 mM Tris-HCl [pH = 8], 150 mM NaCl, 0.5% NP-40, and protease inhibitory cocktail [Roche Applied Science]). After centrifugation, supernatants were incubated for 2 h with poly-U or protein G Sepharose resin (GE Healthcare). After four washes with IP buffer, precipitates were analyzed by immunoblot analysis. Supernatants after centrifugation were used as a positive control (designated Cell lysate in Fig. 4E and 4D).

GST-pull-down assay

GST-pull-down assay was performed as described previously [36].

Supporting Information

Figure S1 Predicted amino acid sequences of CAHL (NM_022828). Underlined residues (LLGQLRA) indicate identical sequence of phage clone #13.
(TIFF)

Figure S2 Indirect immunoflourescence analysis for colocalized with between CAHL and NS3, NS4A, NS4B, NS5A, and NS5B using Huh-7 (A) and MH-14 (B). The primary antibodies used were anti-CAHL (panels a, d, g, j, and m, green) and anti-NS proteins (panels b, e, h, k, and n, red) antibodies. Marge images of green and red signals are shown in panels c, f, i, l, and o.
(TIFF)

Figure S3 Determinant of knockdown efficiency against CAHL gene expression. Five siRNAs for the CAHL gene were individually transfected into MH-14 cells. After transfection, total RNAs of these cells were collected and examined mRNA copy number of CAHL by quantitative real-time RT-PCR.
(TIFF)

Table S1 List of phage clones and their encoding deduced peptide sequences screened by CsA biopanning. *Asterisk indicates the identical sequences.
(DOCX)

Author Contributions

Conceived and designed the experiments: KM HS KW K. Shimotohno SK K. Sakaguchi FS. Performed the experiments: KM HS KW KI TS KK KT HM AT. Analyzed the data: NS. Wrote the paper: KM HS KW FS.

References

1. Calne RY, White DJ, Thiru S, Evans DB, McMaster P, et al. (1978) Cyclosporin-A in patients receiving renal allografts from cadaver donors. Lancet 2: 1323–1327.
2. O'Keefe SJ, Tamura J, Kincaid RL, Tocci MJ, O'Neill EA (1992) FK-506- and CsA-sensitive activation of the interleukin-2 promoter by calcineurin. Nature 357: 692–694.
3. Clipstone NA, Crabtree GR (1992) Identification of calcineurin as a key signalling enzyme in T-lymphocyte activation. Nature 357: 695–697.
4. Liu J, Farmer JD, Jr., Lane WS, Friedman J, Weissman I, et al. (1991) Calcineurin is a common target of cyclophilin-cyclosporin A and FKBP-FK506 complexes. Cell 66: 807–815.
5. Fruman DA, Klee CB, Bierer BE, Burakoff SJ (1992) Calcineurin phosphatase activity in T lymphocytes is inhibited by FK 506 and cyclosporin A. Proc Natl Acad Sci U S A 89: 3686–3690.
6. Fischer G, Tradler T, Zarnt T (1998) The mode of action of peptidylprolyl cis/trans isomerases *in vivo*: binding vs. catalysis. FEBS Lett 426: 17–20.
7. Braaten D, Luban J (2001) Cyclophilin A regulates HIV-1 infectivity, as demonstrated by gene targeting in human T cells. EMBO J 20: 1300–1309.
8. Waldmeier PC, Zimmermann K, Qian T, Tintelnot-Blomley M, Lemasters JJ (2003) Cyclophilin D as a drug target. Curr Med Chem 10: 1485–1506.
9. Hanoulle X, Badillo A, Wieruszeski JM, Verdegem D, Landrieu I, et al. (2009) Hepatitis C virus NS5A protein is a substrate for the peptidyl-prolyl cis/trans isomerase activity of cyclophilins A and B. J Biol Chem 284: 13589–13601.
10. Liu Z, Yang F, Robotham JM, Tang H (2009) Critical role of cyclophilin A and its prolyl-peptidyl isomerase activity in the structure and function of the hepatitis C virus replication complex. J Virol 83: 6554–6565.
11. Watashi K, Ishii N, Hijikata M, Inoue D, Murata T, et al. (2005) Cyclophilin B is a functional regulator of hepatitis C virus RNA polymerase. Mol Cell 19: 111–122.
12. Kuramochi K, Haruyama T, Takeuchi R, Sunoki T, Watanabe M, et al. (2005) Affinity capture of a mammalian DNA polymerase beta by inhibitors immobilized to resins used in solid-phase organic synthesis. Bioconjug Chem 16: 97–104.

13. Aoki S, Morohashi K, Sunoki T, Kuramochi K, Kobayashi S, et al. (2007) Screening of paclitaxel-binding molecules from a library of random peptides displayed on T7 phage particles using paclitaxel-photoimmobilized resin. Bioconjug Chem 18: 1981–1986.
14. Smith GP, Petrenko VA (1997) Phage Display. Chem Rev 97: 391–410.
15. Rodi DJ, Soares AS, Makowski L (2002) Quantitative assessment of peptide sequence diversity in M13 combinatorial peptide phage display libraries. J Mol Biol 322: 1039–1052.
16. Mandava S, Makowski L, Devarapalli S, Uzubell J, Rodi DJ (2004) RELIC–a bioinformatics server for combinatorial peptide analysis and identification of protein-ligand interaction sites. Proteomics 4: 1439–1460.
17. Rodi DJ, Mandava S, Makowski L (2004) DIVAA: analysis of amino acid diversity in multiple aligned protein sequences. Bioinformatics 20: 3481–3489.
18. Makowski L, Rodi DJ (2003) Genome-wide characterisation of the binding repertoire of small molecule drugs. Hum Genomics 1: 41–51.
19. Aoki S, Ohta K, Yamazaki T, Sugawara F, Sakaguchi K (2005) Mammalian mitotic centromere-associated kinesin (MCAK): a new molecular target of sulfoquinovosylacylglycerols novel antitumor and immunosuppressive agents. FEBS J 272: 2132–2140.
20. Morohashi K, Yoshino A, Yoshimori A, Saito S, Tanuma S, et al. (2005) Identification of a drug target motif: an anti-tumor drug NK109 interacts with a PNxxxxP. Biochem Pharmacol 70: 37–46.
21. Kanoh N, Honda K, Simizu S, Muroi M, Osada H (2005) Photo-cross-linked small-molecule affinity matrix for facilitating forward and reverse chemical genetics. Angew Chem Int Ed Engl 44: 3559–3562.
22. Loor F, Tiberghien F, Wenandy T, Didier A, Traber R (2002) Cyclosporin: structure-activity relationships for the inhibition of the human FPR1 formyl peptide receptor. J Med Chem 45: 4613–4628.
23. Yang F, Robotham JM, Nelson HB, Irsigler A, Kenworthy R, et al. (2008) Cyclophilin A is an essential cofactor for hepatitis C virus infection and the principal mediator of cyclosporine resistance in vitro. J Virol 82: 5269–5278.
24. Chatterji U, Bobardt M, Selvarajah S, Yang F, Tang H, et al. (2009) The isomerase active site of cyclophilin A is critical for hepatitis C virus replication. J Biol Chem 284: 16998–17005.
25. Fernandes F, Poole DS, Hoover S, Middleton R, Andrei AC, et al. (2007) Sensitivity of hepatitis C virus to cyclosporine A depends on nonstructural proteins NS5A and NS5B. Hepatology 46: 1026–1033.
26. Robida JM, Nelson HB, Liu Z, Tang H (2007) Characterization of hepatitis C virus subgenomic replicon resistance to cyclosporine in vitro. J Virol 81: 5829–5840.
27. Bouchard R, Bailly A, Blakeslee JJ, Oehring SC, Vincenzetti V, et al. (2006) Immunophilin-like TWISTED DWARF1 modulates auxin efflux activities of Arabidopsis P-glycoproteins. J Biol Chem 281: 30603–30612.
28. Flisiak R, Feinman SV, Jablkowski M, Horban A, Kryczka W, et al. (2009) The cyclophilin inhibitor Debio 025 combined with PEG IFNalpha2a significantly reduces viral load in treatment-naïve hepatitis C patients. Hepatology 49: 1460–1468.
29. Ariumi Y, Kuroki M, Abe K, Dansako H, Ikeda M, et al. (2007) DDX3 DEAD-box RNA helicase is required for hepatitis C virus RNA replication. J Virol 81: 13922–13926.
30. Jangra RK, Yi M, Lemon SM (2010) Regulation of hepatitis C virus translation and infectious virus production by the microRNA miR-122. J Virol 84: 6615–6625.
31. Goh PY, Tan YJ, Lim SP, Tan YH, Lim SG, et al. (2004) Cellular RNA helicase p68 relocalization and interaction with the hepatitis C virus (HCV) NS5B protein and the potential role of p68 in HCV RNA replication. J Virol 78: 5288–5298.
32. Larrea E, Garcia N, Qian C, Civera MP, Prieto J (1996) Tumor necrosis factor a gene expression and the response to interferon in chronic hepatitis C. Hepatology 23: 210–217.
33. Okanami M, Meshi T, Iwabuchi M (1998) Characterization of a DEAD box ATPase/RNA helicase protein of *Arabidopsis thaliana*. Nucleic Acids Res 26: 2638–2643.
34. Watashi K, Hijikata M, Hosaka M, Yamaji M, Shimotohno K (2003) Cyclosporin A suppresses replication of hepatitis C virus genome in cultured hepatocytes. Hepatology 38: 1282–1288.
35. Imai A, Sahara H, Tamura Y, Jimbow K, Saito T, et al. (2007) Inhibition of endogenous MHC class II-restricted antigen presentation by tacrolimus (FK506) via FKBP51. Eur J Immunol 37: 1730–1738.
36. Watashi K, Hijikata M, Tagawa A, Doi T, Marusawa H, et al. (2003) Modulation of retinoid signaling by a cytoplasmic viral protein via sequestration of Sp110b, a potent transcriptional corepressor of retinoic acid receptor, from the nucleus. Mol Cell Biol 23: 7498–7509.

Biochemical and Biophysical Research Communications 415 (2011) 714–719

Contents lists available at SciVerse ScienceDirect

Biochemical and Biophysical Research Communications

journal homepage: www.elsevier.com/locate/ybbrc

Potent and selective inhibition of hepatitis C virus replication by novel phenanthridinone derivatives

Mohammed T.A. Salim [a], Hiroshi Aoyama [b,1], Kazuyuki Sugita [b], Kouichi Watashi [c], Takaji Wakita [c], Takayuki Hamasaki [a], Mika Okamoto [a], Yasuo Urata [d], Yuichi Hashimoto [b], Masanori Baba [a,*]

[a] Division of Antiviral Chemotherapy, Center for Chronic Viral Diseases, Graduate School of Medical and Dental Sciences, Kagoshima University, 8-35-1, Sakuragaoka, Kagoshima 890-8544, Japan
[b] Institute of Molecular and Cellular Biosciences, The University of Tokyo, Tokyo 113-0032, Japan
[c] Department of Virology II, National Institute of Infectious Diseases, Tokyo 162-8640, Japan
[d] Oncolys BioPharma Inc., Tokyo 105-0001, Japan

ARTICLE INFO

Article history:
Received 24 October 2011
Available online 9 November 2011

Keywords:
Flavivirus
HCV
Phenanthridinone
Replicon cell
JFH1

ABSTRACT

A number of novel phenanthridinone derivatives were examined for their inhibitory effect on hepatitis C virus (HCV) replication in Huh-7 cells harboring self-replicating subgenomic viral RNA replicons with a luciferase reporter (LucNeo#2). The activity of compounds was further confirmed by inhibition of viral RNA copy number in different subgenomic and full-genomic replicon cells using real-time reverse transcription polymerase chain reaction. Among the compounds, 4-butyl-11-(1,1,1,3,3,3-hexafluoro-2-hydroxypropan-2-yl)-7-methoxy-[1,3]dioxolo[4,5-*c*]phenanthridin-5(4*H*)-one (HA-719) was found to be the most active with a 50% effective concentration of 0.063 ± 0.010 μM in LucNeo#2 cells. The compound did not show apparent cytotoxicity to the host cells at concentrations up to 40 μM. Western blot analysis demonstrated that HA-719 reduced the levels of NS3 and NS5A proteins in a dose-dependent fashion in the replicon cells. Interestingly, the phenanthridinone derivatives including HA-719 were less potent inhibitors of JFH1 strain (genobtype 2a HCV) in cell-free virus infection assay. Although biochemical assays revealed that HA-719 proved not to inhibit NS3 protease or NS5B RNA polymerase activity at the concentrations capable of inhibiting viral replication, their molecular target (mechanism of inhibition) remains unknown. Considering the fact that most of the anti-HCV agents currently approved or under clinical trials are protease and polymerase inhibitors, the phenanthridinone derivatives are worth pursuing for their mechanism of action and potential as novel anti-HCV agents.

1. Introduction

Hepatitic C virus (HCV) infection is a worldwide problem. More than 130 million individuals are infected with this virus, and 3–4 million are newly infected every year. In general, HCV infection proceeds to chronic infection [1], which often induces liver cirrhosis and hepatocellular carcinoma [2] liver transplantation is the only way to rescue patients with the end-stage liver disorders caused by HCV infection [3]. Protective vaccines are not available so far, and pegylated interferon (PEG-IFN) and the nucleoside analog ribavirin are the standard treatment for HCV infection [4–6]. However, many patients cannot tolerate the serious side effects of PEG-IFN and ribavirin. Therefore, the development of novel agents with better efficacy and tolerability is still mandatory.

HCV is an enveloped virus belonging to the hepacivirus genus of the family *Flaviviridae* [7,8]. The viral genome consists of positive sense single RNA coding a polyprotein cleaved by viral and host proteases into four structural and six non-structural proteins. Non-structural proteins are involved in the replication of HCV genome [9]. The discovery of effective anti-HCV agents was greatly hampered by the lack of cell culture systems that allowed robust propagation of HCV in laboratories. However, the development of HCV RNA replicon systems [10] and recent success in propagating infectious virus particles in vitro have provided efficient tools for screening new antiviral agents against HCV replication [11,12]. Furthermore, replicons containing a reporter gene, such as luciferase and green fluorescence protein, have provided fast and reproducible screening of a large number of compounds for their antiviral activity [13–15].

Currently, two NS3 protease inhibitors, teraprevir and boceprevir, have been licensed and a considerable number of novel anti-HCV agents are under clinical trials [16,17]. Most of them are directly acting inhibitors of NS3 protease or NS5B polymerase. However, the

* Corresponding author. Fax: +81 99 275 5932.
E-mail address: m-baba@m2.kufm.kagoshima-u.ac.jp (M. Baba).
[1] Present address: School of Pharmacy, Tokyo University of Pharmacy and Life Sciences, Tokyo 192-0392, Japan.

0006-291X/$ - see front matter © 2011 Elsevier Inc. All rights reserved.
doi:10.1016/j.bbrc.2011.10.153

emergence of HCV mutants resistant to most of these agents has also been reported [18]. To circumvent the drug-resistance, it seems necessary to use more than two directly acting drugs targeting different molecules for inhibition of viral replication [19]. Thus, in addition to the protease and polymerase inhibitors, novel compounds with a unique mechanism of action are highly desired.

We have recently identified some compounds with a novel phenanthridinone structure as moderate inhibitors of HCV replication [20]. This prompted us to synthesize a number of phenanthridinone derivatives and investigate their anti-HCV activity. After optimization of chemical structures, we have obtained the compounds that exert anti-HCV activity in the nanomolar range. Interestingly, these compounds did not inhibit the enzymatic activity of NS3 protease or NS5B RNA polymerase at the concentrations capable of inhibiting HCV replication in replicon cells.

2. Materials and methods

2.1. Compounds

More than 100 phenanthridinone derivatives were synthesized and used in this study. The synthesis of these compounds has been described previously [20,21]. Cyclosporin A (CsA) was purchased from Sigma–Aldrish. All compounds were dissolved in dimethyl sulfoxide (DMSO) (Nacalai Tesque) at a concentration of 20 mM or higher to exclude the cytotoxicity of DMSO and stored at −20 °C until use.

2.2. Cells

Huh-7 cells were grown and cultured in Dulbecco's modified Eagle medium with high glucose (Gibco/BRL) supplemented with 10% heat-inactivated fetal bovine serum (Gibco/BRL), 100 U/ml penicillin G, and 100 μg/ml streptomycin. Huh-7 cells containing self-replicating subgenomic HCV replicons with a luciferase reporter, LucNeo#2 [22], were maintained in culture medium containing 1 mg/ml G418 (Nakarai Tesque). The subgenomic replicon cells without reporter #50-1 and the full-genomic replicon cells NNC#2 [23] were kindly provided by Dr. Hijikata (Kyoto University, Kyoto, Japan). These cells were also maintained in culture medium containing 1 mg/ml G418.

2.3. Anti-HCV assays

The anti-HCV activity of the test compounds was determined in LucNeo#2 cells by the previously described method with some modifications [24]. Briefly, the cells (5×10^3 cells/well) were cultured in a 96-well plate in the absence of G418 and in the presence of various concentrations of the compounds. After incubation at 37 °C for 3 days, the culture medium was removed, and the cells were washed twice with phosphate-buffered saline (PBS). Lysis buffer was added to each well, and the lysate was transferred to the corresponding well of a non-transparent 96-well plate. The luciferase activity was measured by addition of the luciferase reagent in a luciferase assay system kit (Promega) using a luminometer with automatic injectors (Berthold Technologies).

The activity of the test compounds was also determined by the inhibition of HCV RNA synthesis in LucNeo#2, #50–1, and NNC#2 cells [23,25]. The cells (5×10^3 cells/well) were cultured in a 96-well plate in the absence of G418 and in the presence of various concentrations of the compounds. After incubation at 37 °C for 3 days, the cells were washed with PBS, treated with lysis buffer in TaqMan® Gene Expression Cell-to-CT™ kit (Applied Biosystems), and the lysate was subjected to real-time reverse transcription polymerase chain reaction (RT-PCR), according to the manufacturer's instructions. The 5′-untranslated region of HCV RNA was quantified using the sense primer 5′-CGGGAGAGCCATAGTGG-3′, the antisense primer 5′-AGTACCACAAGGCCTTTCG-3′, and the fluorescence probe 5′-CTGCGGAACCGGTGAGTACAC-3′ (Applied Biosystems).

The inhibitory effect of the test compounds on the replication of a genotype 2a strain was evaluated by the infection of Huh-7.5.1 cells, kindly provided by Dr. Chisari at Scripps Institute, with cell-free JFH-1 virus, as previously described [11]. At 48 h after virus infection, the cells were treated with SideStep Lysis and Stabilization Buffer (Agilent Technologies), and the lysate was subjected to real-time RT-PCR for quantification of HCV RNA [25].

2.4. Cytotoxicity assay

Huh-7 cells (5×10^3 cells/well) were cultured in a 96-well plate in the presence of various concentrations of the test compounds. After incubation at 37 °C for 3 days, the number of viable cells was determined by a dye method using the water soluble tetrazolium Tetracolor One® (Seikagaku Corporation), according to the manufacturer's instructions. The cytotoxicity of the compounds was also evaluated by the inhibition of host cellular mRNA synthesis. The cells were treated with lysis buffer in the kit, as described above, and the cell lysate was subjected to real-time RT-PCR for amplification of a part of glyceraldehyde-3-phosphate dehydrogenase (GAPDH) RNA using a TaqMan® RNA control reagent (Applied Biosystems).

2.5. Immunoblotting

LucNeo#2 cells (5×10^3 cells/well) were cultured in a 96-well plate in the presence of various concentrations of the test compounds. After incubation at 37 °C for 4 days, the culture medium was removed, and the cells were washed with PBS and treated with lysis buffer (RIPA Buffer®, Funakoshi). The protein concentration of the lysate was measured by Bradford protein assay method (Bio-Rad). Then, the lysate was subjected to sodium dodecyl sulfate polyacrylamide gel electrophoresis (SDS–PAGE). The primary antibodies used for protein detection were anti-NS3 (Thermo Scientific), anti-NS5A (Acris Antibodies), and anti-GAPDH (Santa Cruz Biotechnology) mouse monoclonal antibodies.

2.6. Protease and polymerase inhibition assays

The effect of the test compounds on NS3 protease activity was determined by a fluorescence resonance energy transfer-based assay using SensoLyte® 520 HCV Assay Kit (AnaSpec), according to the manufacturer's instructions. The inhibition assay for NS5B polymerase was performed at 37 °C for 60 min in a 384-well plate. A reaction mixture (30 μl/well) contains 20 mM Tris–HCl (pH 7.6), 10 mM $MgCl_2$, 20 mM NaCl, 1 mM dithiothreitol, 0.05% Tween 20, 0.05% pluronic F127, 1 μM [^{3}H]GTP (0.1 μCi/well) plus cold GTP, 5 nM poly(rC), 62.5 nM biotinylated dG_{12}, 45 nM recombinant NS3 protease, and various concentrations of the compounds. The reaction was stopped by streatavidin scintillation proximity assay beads in 0.5 M ethylenediaminetetraacetic acid. The plate was counted with a microbeta reader on the following day.

3. Results

When a number of phenanthridinone derivatives were examined for their antiviral activity in LucNeo#2 cells, three phenanthridinone derivatives, 5-butyl-2-(1,1,1,3,3,3-hexafluoro-2-hydroxypropan-2-yl)-3,8-dimethoxyphenanthridin-6(5*H*)-one (KZ-16), 4-butyl-11-(1,1,1,3,3,3-hexafluoro-2-hydroxypropan-2-yl)-[1,3]dioxolo[4,5-*c*]

phenanthridin-5(4*H*)-one (HA-718), and 4-butyl-11-(1,1,1,3,3,3-hexafluoro-2-hydroxypropan-2-yl)-[1,3]dioxolo[4,5-*c*]phenanthridin-5(4*H*)-one (HA-718), and 4-butyl-11-(1,1,1,3,3,3-hexafluoro-2-hydroxypropan-2-yl)-7-methoxy-[1,3]dioxolo[4,5-*c*] phenanthridin-5(4*H*)-one (HA-719) (Fig. 1) proved to be highly potent and selective inhibitors of HCV (genotype 1b) replication. KZ-16, HA-718, and HA-719 reduced luciferase activity and viral RNA copy number in LucNeo#2 cells in a dose-dependent fashion (Fig. 2A–C). However, they did not affect the viability of Huh-7.5.1 cells at concentrations up to 40 μM (Fig. 2D). When the cytotoxicity of the compounds was evaluated by the copy number of GAPDH mRNA in the host cells, a similar result was obtained (data not shown).

Table 1 summarizes the anti-HCV activity of KZ-16, HA-718, and HA-719 in different (genotype 1b) replicon cells and in Huh-7 cells infected with cell-free JFH1 (genotype 2a) virus. The highest activity was achieved by HA-719 followed by KZ-16 and HA-718. The EC_{50} of KZ-16, HA-718, and HA-719 were 0.13 ± 0.04, 0.23 ± 0.06, and 0.063 ± 0.010 μM, respectively, in LucNeo#2 cells, when determined by the luciferase reporter activity. The 50% cytotoxic concentrations (CC_{50}) of all compounds were >40 μM. Therefore, the selectivity indices (SI), based on the ratio of CC_{50} to EC_{50}, of KZ-16, HA-718, and HA-719 were >307, >173, and >634, respectively. The anti-HCV activity of these compounds was confirmed by reduction of the viral RNA copy number in different replicon cells. However, they were less potent inhibitors of genotype 2a HCV (JFH1) replication in cell-free virus infection assay. Furthermore, the phenanthridinone derivatives were much less active in Huh-7 cells transfected with JFH1 replicons than in genotype 1b replicon cells (data not shown).

Immunoblot analysis was conducted to confirm that phenanthridinone derivatives were inhibitory to the expression of NS3 and NS5A proteins of HCV. As shown in Fig. 3, HA-719 strongly inhibited NS3 and NS5A expression in LucNeo#2 cells in a dose dependent fashion without affecting the expression of the host cellular protein GAPDH. The compound achieved 93% and 86% inhibition of NS3 and NS5A, respectively, at a concentration of 0.5 μM, indicating that HA-719 is a potent inhibitor of HCV protein expression as well as viral RNA synthesis. Immunoblot analysis was also conducted for another phenanthridinone derivative, 2-(2-benzyloxy-1,1,1,3,3,3-hexafluoropropan-2-yl)-5-butyl-3-methoxyphenanthridin-6(5*H*)-one (KZ-37), of which anti-HCV activity was weaker than HA-719. KZ-37 also proved inhibitory to NS3 and NS5A expression in a dose-dependent fashion (data not shown).

In our attempt to elucidate the mechanism of action of the compounds, HA-719 was examined for their ability to inhibit the enzymatic activity of genotype 1b NS3 protease and NS5B polymerase in cell-free assay systems. Little, if any, inhibition of NS3 protease activity was observed for HA-719. Its 50% inhibitory concentration (IC_{50}) for the protease was 5.7 μM (data not shown), which was much higher than its EC_{50} for HCV replication in replicon cells (0.063–0.44 μM). HA-719 did not show any inhibitory effect on NS5B polymerase activity at concentrations up to 20 μM (data not shown). Furthermore, KZ-37, of which EC_{50} for HCV replication was 2.1–4.8 μM, was inactive against these two enzymes at a concentration of 20 μM (data not shown). Thus, it is unlikely that the phenanthridinone derivatives suppress HCV replication by inhibiting the activity of either NS3 protease or NS5B polymerase.

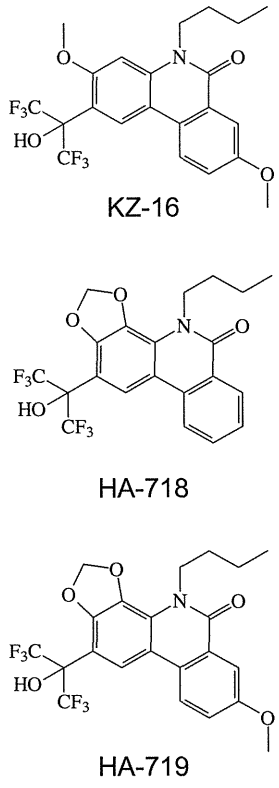

Fig. 1. Chemical structures of phenanthridinone derivatives.

4. Discussion

In this study, we have demonstrated that novel phenanthridinone derivatives are potent and selective inhibitors of HCV replication in vitro. Our previous study on the synthesis and antiviral activity of phenanthridinone derivatives demonstrated that some of them exhibited selective but moderate activity against HCV replication in replicon cells [20,21]. After optimization of chemical structures, we succeeded in obtaining a series of potent and selective derivatives (Fig. 1). Among them, the most active one was HA-719, a novel phenanthridinone derivative with a dioxole structure.

Previous studies of HCV replicon cell systems indicated that most replicons had cell culture-adaptive mutations, which arose during the selection process with G418 and enhanced replication efficiency [26–29]. Self-replicating subgenomic RNA replicons could be eliminated from Huh-7 cells by prolonged treatment with IFN, and a higher frequency of cured cells could support the replication of subgenomic and full-genomic replicons [30]. The replication efficiency decreased with increasing amounts of transfected replicon RNA, indicating that viral RNA or proteins are cytopathic or that host cell factors in Huh-7 cells limit RNA amplification [31]. Therefore, both viral and cellular factors are considered to be important determinants for the efficiency of HCV replication in cell cultures, which may be able to explain the difference in EC_{50} values of the compounds among the subgenomic replicon cells used in this study (Table 1). Similarly, the difference in EC_{50} values in subgenomic and full-genomic replicon cells might be due to the difference of HCV RNA length or the difference of the host cells [32]. In fact, shorter RNA is known to replicate more efficiently than longer one [33].

The activity of phenanthridinone derivatives against the genotype 2a strain JFH1 was weaker than that against genotype 1b (Table 1). Although the assay systems were not the same (replicon cell assay for genotype 1b versus cell-free virus infection assay for genotype 2b), the compounds were much less active against genotype 2a (Table 1 and data not shown). Such difference in drug-sensitivity between genotype 1b and genotype 2a was previously reported and attributed to the genetic heterogeneity within the HCV genome [23]. In addition, the anti-HCV activity of compounds had been optimized in the genotype 1b replicon cells. HCV is classified into 6 genotypes that are further separated into a series of subtypes [34,35]. Among the genotypes, genotype 1b virus is epidemiologically predominant in Japan, and 65 and 17% of the cases

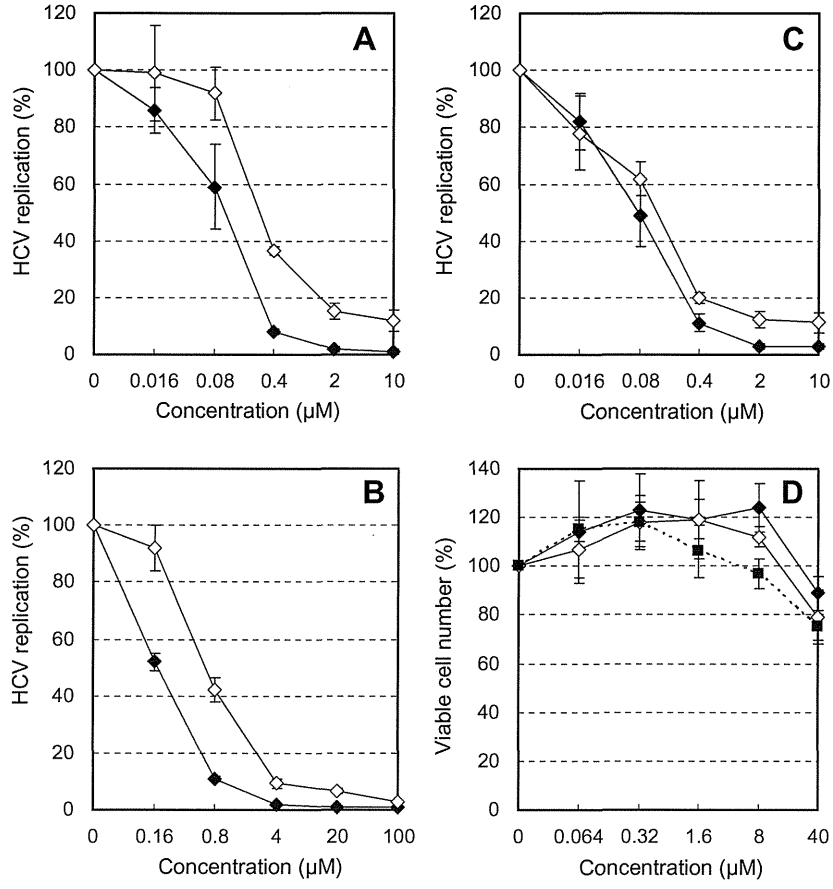

Fig. 2. Inhibitory effect of phenanthridinone derivatives on the replication HCV RNA replicons in LucNeo#2 cells and the proliferation of Huh-7 cells. LucNeo#2 cells were cultured in the presence of various concentrations of (A) KZ-16, (B) HA-718, or (C) HA-719. After incubation for 3 days, the cells were subjected to luciferase assay (closed diamond) and real-time RT-PCR (open diamond) to measure replicon-associated luciferase activity and RNA copy number, respectively, as parameters of HCV replication. (D) For the cell proliferation assay, Huh-7 cells were cultured in the presence of various concentrations of KZ-16 (closed diamond), HA-718 (open diamond), or HA-719 (closed square). After incubation for 3 days, the number of viable cells was determined by a tetrazolium dye method. Data represent means ± SD for triplicates experiments. Experiments were repeated at least twice, and a representative result is shown.

Table 1
Anti-HCV activity of phenanthridinone derivatives.

Compound		EC_{50} (μM)					CC_{50} (μM)
	Virus genotype	1b				2a	
	Cell	LucNeo#2		#50-1	NNC#2	Huh-7.5.1	Huh-7
	Assay	Luciferase	Real-time RT-PCR				Tetrazolium
KZ-16		0.13 ± 0.04	0.28 ± 0.01	0.40 ± 0.12	0.40 ± 0.14	2.6 ± 0.9	>40
HA-718		0.23 ± 0.06	0.68 ± 0.02	0.97 ± 0.56	0.90 ± 0.44	14 ± 5	>40
HA-719		0.063 ± 0.010	0.14 ± 0.01	0.25 ± 0.05	0.44 ± 0.20	4.9 ± 2.2	>40
CsA		0.24 ± 0.05	0.16 ± 0.01	0.18 ± 0.03	N.D.	0.58 ± 0.01	12 ± 3

EC_{50}: 50% effective concentration; CC_{50}: 50% cytotoxic concentration. N.D.: not determined.
Antiviral assay against the genotype 2a HCV was evaluated by the infection of Huh-7.5.1 cells with cell-free JFH-1 virus (see Section 2).
Except for the results in NNC#2 cells, all data represent means ± SD for three independent experiments. The data in NNC#2 cells represent means ± ranges for two independent experiments.

of HCV-related chronic hepatitis were caused by genotype 1b and genotype 2b, respectively [36].

At present, the target molecule of our phenanthridinone derivatives for inhibition of HCV replication remains unknown. Although it cannot be completely excluded that the compounds are inhibitors of NS3 protease or NS5B polymerase, biochemical assays revealed that HA-719 proved not to inhibit the activity of these enzymes at the concentrations capable of inhibiting viral replication. Therefore, the compounds may interact with another non-structural protein essential for viral replication, such as NS3 helicase and NS5A. In fact, a highly active inhibitor targeting NS5A has recently been identified [37]. Alternatively, the phenanthridinone derivatives may inhibit HCV replication through the interaction with host cellular factors deeply involved in HCV replication process [38–40]. It was reported that PJ34, a phenanthridinone derivative, had immunomodulatory activities and was protective against autoimmune diabetes [41], liver cancer [42], and stroke [43]. These studies suggested that the effects of PJ34 were attributed to the inhibition of poly(ADP-ribose) polymerase (PARP). Therefore, HA-719 was tested for its inhibitory effect on

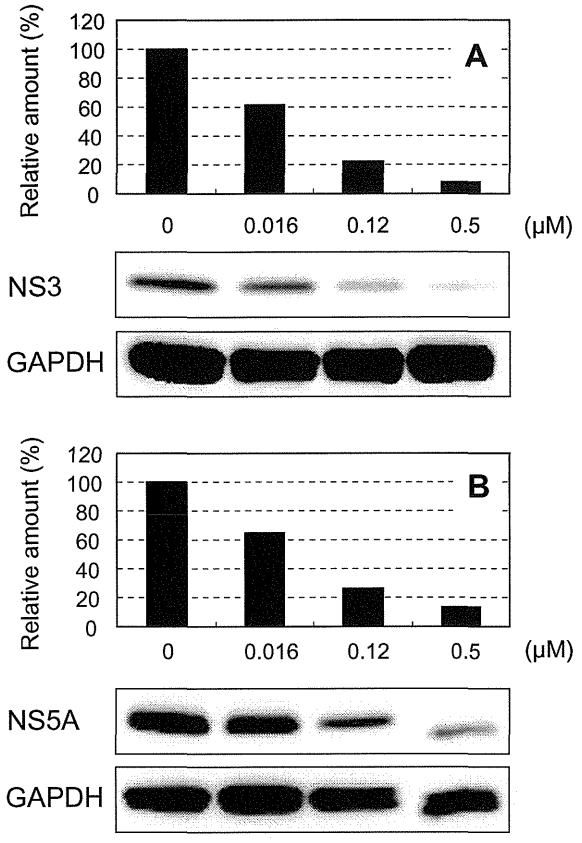

Fig. 3. Inhibitory effect of HA-719 on the expression of HCV proteins in LucNeo#2 cells. The cells were cultured in the presence of various concentrations of the compound. After incubation for 4 days, the cells were subjected to electrophoresis and immunoblot analysis for expression of (A) NS3 and (B) NS5A proteins. The band images were quantified by an image scanner and densitometer. Experiments were repeated at least twice, and a representative result is shown.

PARP activity and found to be inactive (data not shown). It was reported that some phenanthridinone derivatives had anti-human immunodeficiency virus (HIV) activity through the inhibition of viral integrase [44]. However, our compounds did not show selective inhibition of HIV replication in cell cultures (data not shown). Further studies, including the establishment of drug-resistant replicons, are in progress to determine the mechanism of action of the phenanthridinone derivatives.

In conclusion, our results clearly demonstrate that the novel phenanthridinone derivatives, especially HA-719, are highly potent and selective inhibitors of HCV replication in vitro. Although further studies, such as determination of their target molecule and pharmacological properties in vivo, are required, this class of compounds should be pursued for their clinical potential in the treatment of HCV infection.

Acknowledgments

This work was supported by the Science and Technology Incubation Program in Advanced Regions, Japan Science and Technology Agency (JST), Japan. We thank the Egyptian Government for support to M.T.A. Salim, who was previously an assistant lecturer in the Faculty of Pharmacy, Al-Azhar University, Egypt and is currently a postgraduate student of Kagoshima University, Japan.

References

[1] M. Koziel, M. Peters, Viral hepatitis in HIV infection, N. Engl. J. Med. 356 (2007) 1445–1454.
[2] J.H. Hoofnagle, Course and outcome of hepatitis C, Hepatology 36 (2002) S21–29.
[3] P. Sharma, A. Lok, Viral hepatitis and liver transplantation, Semin. Liver Dis. 26 (2006) 285–297.
[4] A.M. Di Bisceglie, J.H. Hoofnagle, Optimal therapy of hepatitis C, Hepatology 36 (2002) S121–127.
[5] M.W. Fried, M.L. Shiffman, K.R. Reddy, C. Smith, G. Marinos, F.L. Jr Gonçales, D. Häussinger, M. Diago, G. Carosi, D. Dhumeaux, A. Craxi, A. Lin, J. Hoffman, J. Yu, Peginterferon alfa-2a plus ribavirin for chronic hepatitis C virus infection, N. Engl. J. Med. 347 (2002) 975–982.
[6] A. Craxi, A. Licata, Clinical trial results of peginterferons in combination with ribavirin, Semin. Liver Dis. 23 (1) (2003) 35–46.
[7] Q.L. Choo, G. Kuo, A.J. Weiner, L.R. Overby, D.W. Bradley, M. Houghton, Isolation of a cDNA clone derived from a blood-borne non-A, Non-B viral hepatitis genome, Science 244 (1989) 359–362.
[8] M. Houghton, A. Weiner, J. Han, G. Kuo, Q.L. Choo, Molecular biology of the hepatitis C viruses: implications for diagnosis. Development and control of viral disease, Hepatology 14 (1991) 381–388.
[9] T. Suzuki, K. Ishii, H. Aizaki, T. Wakita, Hepatitis C viral life cycle, Adv. Drug Deliv. Rev. 59 (2007) 1200–1212.
[10] V. Lohmann, F. Korner, J.O. Koch, U. Herian, L. Theilmann, R. Bartenschlager, Replication of subgenomic hepatitis C virus RNAs in a hepatoma cell line, Science 285 (1999) 110–113.
[11] T. Wakita, T. Pietschmann, T. Kato, T. Date, M. Miyamoto, Z. Zhao, K. Murthy, A. Habermann, H.G. Krausslich, M. Mizokami, R. Bartenschlager, T.J. Liang, Production of infectious hepatitis C virus in tissue culture from a cloned viral genome, Nat. Med. 11 (2005) 791–796.
[12] M.B. Zeisel, T.F. Baumert, Production of infectious hepatitis C virus in tissue culture: a breakthrough for basic and applied research, J. Hepatol. 44 (2006) 436–439.
[13] R. Bartenschlager, The hepatitis C virus replicon system: from basic research to clinical application, J. Hepatol. 43 (2005) 210–216.
[14] R. Bartenschlager, Hepatitis C virus molecular clones: from cDNA to infectious virus particles in cell culture, Curr. Opin. Microbiol. 9 (2006) 416–422.
[15] V. Brass, D. Moradpour, H.E. Blum, Molecular virology of hepatitis C virus (HCV): 2006 update, Int. J. Med. Sci. 3 (2006) 29–34.
[16] L. Delang, L. Coelmont, J. Neyts, Antiviral therapy for hepatitis C virus: beyond the standard of care, Viruses 2 (2010) 826–866.
[17] C.M. Lange, C. Sarrazin, S. Zeuzem, Specifically targeted anti-viral therapy for hepatitis C – A new era in therapy, Aliment. Pharmacol. Ther. 32 (2010) 14–28.
[18] R.F. Schinazi, L. Bassit, C. Gavegnano, HCV drug discovery aimed at viral eradication, J. Viral Hepat. 17 (2010) 77–90.
[19] T.L. Kieffer, A.D. Kwong, G.R. Picchio, Viral resistance to specifically targeted antiviral therapies for hepatitis C (STAT-Cs), J. Antimicrob. Chemother. 65 (2010) 202–212.
[20] M. Nakamura, A. Aoyama, M.T.A. Salim, M. Okamoto, M. Baba, H. Miyachi, Y. Hashimoto, H. Aoyama, Structural development studies of anti-hepatitis C virus agents with a phenanthridinone skeleton, Bioorg. Med. Chem. 18 (2010) 2402–2411.
[21] H. Aoyama, K. Sugita, M. Nakamura, A. Aoyama, M.T.A. Salim, M. Okamoto, M. Baba, Y. Hashimoto, Fused heterocyclic amido compounds as anti-hepatitis C virus agents, Bioorg. Med. Chem. 19 (2011) 2675–2687.
[22] K. Goto, K. Watashi, T. Murata, T. Hishiki, M. Hijikata, K. Shimotohno, Evaluation of anti-hepatitis C virus effects of cyclophilin inhibitors, cyclosporine A, and NIM811, Biochem. Biophys. Res. Commun. 343 (2006) 879–884.
[23] N. Ishii, K. Watashi, T. Hishiki, K. Goto, D. Inoue, M. Hijikata, T. Wakita, N. Kato, K. Shimotohno, Diverse effects of cyclosporine on hepatitis C virus strain replication, J. Virol. 80 (2006) 4510–4520.
[24] M.P. Windisch, M. Frese, A. Kaul, M. Trippler, V. Lohmann, R. Bartenschlager, Dissecting the interferon-induced inhibition of hepatitis C virus replication by using a novel host cell line, J. Virol. 79 (2005) 13778–13793.
[25] K. Watashi, M. Hijikata, M. Hosaka, M. Yamaji, K. Shimotohno, Cyclosporine A suppresses replication of hepatitis C virus genome in cultured hepatocytes, Hepatology 38 (2003) 1282–1288.
[26] N. Appel, T. Pietschmann, R. Bartenschlager, Mutational analysis of hepatitis C virus nonstructural protein 5A: potential role of differential phosphorylation in RNA replication and identification of a genetically flexible domain, J. Virol. 79 (2005) 3187–3194.
[27] M. Ikeda, M. Yi, K. Li, S.M. Lemon, Selectable subgenomic and genome-length dicistronic RNAs derived from an infectious molecular clone of the HCV-N strain of hepatitis C virus replicate efficiently in cultured Huh7cells, J. Virol. 76 (2002) 2997–3006.
[28] M. Ikeda, K. Abe, H. Dansako, T. Nakamura, K. Naka, N. Kato, Efficient replication of a full-length hepatitis C virus genome, Strain O, in cell culture, and development of a luciferase reporter system, Biochem. Biophys. Res. Commun. 329 (2005) 1350–1359.
[29] M. Yi, S.M. Lemon, Adaptive mutations producing efficient replication of genotype 1a hepatitis C virus RNA in normal Huh7 cells, J. Virol. 78 (2004) 7904–7915.
[30] K.J. Blight, J.A. McKeating, C.M. Rice, Highly permissive cell lines for subgenomic and genomic hepatitis C virus RNA replication, J. Virol. 76 (2002) 13001–13014.
[31] V. Lohmann, S. Hoffmann, U. Herian, F. Penin, R. Bartenschlager, Viral and cellular determinants of hepatitis C virus RNA replication in cell culture, J. Virol. 77 (2003) 3007–3019.

[32] K. Abe, M. Ikeda, H. Dansako, K. Naka, N. Kato, Cell culture-adaptive NS3 mutations required for the robust replication of genome-length hepatitis C virus RNA, Virus Res. 125 (2007) 88–97.
[33] M. Rychlowska, K. Bieńkowska-Szewczyk, Hepatitis C – new developments in the studies of the viral life cycle, Acta Biochim. Pol. 54 (2007) 703–715.
[34] J. Bukh, R.H. Purcell, R.H. Miller, Sequence analysis of the core gene of 14 hepatitis C virus genotypes, Proc. Natl. Acad. Sci. USA 91 (1994) 8239–8243.
[35] O. Ohno, M. Mizokami, R.R. Wu, M.G. Saleh, K. Ohba, E. Orito, M. Mukaide, R. Williams, J.Y. Lau, New hepatitis C virus (HCV) genotyping system that allows for identification of HCV genotypes 1a, 1b, 2a, 2b, 3a, 3b, 4, 5a, and 6a, J. Clin. Microbiol. 35 (1997) 201–207.
[36] T. Kato, T. Date, M. Miyamoto, A. Furusaka, K. Tokushige, M. Mizokami, T. Wakita, Efficient replication of the genotype 2a hepatitis C virus subgenomic replicon, Gastroenterology 125 (2003) 1808–1817.
[37] M. Gao, R.E. Nettles, M. Belema, L.B. Snyder, V.N. Nguyen, R.A. Fridell, M.H. Serrano-Wu, D.R. Langley, J.H. Sun, D.R.I.I. O'Boyle, J.A. Lemm, C. Wang, J.O. Knipe, C. Chien, R.J. Colonno, D.M. Grasela, N.A. Meanwell, L.G. Hamann, Chemical genetics strategy identifies an HCV NS5A inhibitor with a potent clinical effect, Nature 465 (2010) 96–100.
[38] L. Coelmont, S. Kaptein, J. Paeshuyse, I. Vliegen, J.M. Dumont, G. Vuagniaux, J. Neyts, Debio 025, a cyclophilin binding molecule, is highly efficient in clearing hepatitis C virus (HCV) replicon-containing cells when used alone or in combination with specifically targeted antiviral therapy for HCV (STAT-C) inhibitors, Antimicrob. Agents. Chemother. 53 (2009) 967–976.
[39] P. Georgel, C. Schuster, M.B. Zeisel, F. Stoll-Keller, T. Berg, S. Bahram, T.F. Baumert, Virus-host interactions in hepatitis C virus infection: implications for molecular pathogenesis and antiviral strategies, Trends Mol. Med. 16 (2010) 277–286.
[40] T. Suzuki, A Hepatitis C virus-host interaction involved in viral replication: toward the identification of antiviral targets, Jpn. J. Infect. Dis. 63 (2010) 307–311.
[41] W.L. Suarez-Pinzon, J.G. Mabley, R. Power, C. Szabó, A. Rabinovitch, Poly (ADP-ribose) polymerase inhibition prevents spontaneous and recurrent autoimmune diabetes in NOD mice by inducing apoptosis of islet-infiltrating leukocytes, Diabetis 52 (2003) 1683–1688.
[42] S.H. Huang, M. Xiong, X.P. Chen, Z.Y. Xiao, Y.F. Zhao, Z.Y. Huang, PJ34, an inhibitor of PARP-1, Suppresses cell growth and enhances the suppressive effects of cisplatin in liver cancer cells, Oncol. Rep. 20 (2008) 567–572.
[43] G.E. Abdelkarim, K. Gertz, C. Harms, J. Katchanov, U. Dirnagl, C. Szabó, M. Endres, Protective effects of PJ34, a novel, potent inhibitor of poly(ADP-ribose) polymerase (PARP) in vitro and in vivo models of stroke, Int. J. Mol. Med. 7 (2001) 255–260.
[44] S. Patil, S. Kamath, T. Sanchez, N. Neamati, R.F. Schinazi, J.K. Buolamwini, Synthesis and biological evaluation of novel 5(*H*)-phenanthridin-6-ones, 5(*H*)-phenanthridin-6-one diketo acid, and polycyclic aromatic diketo acid analogs as new HIV-1 integrase inhibitors, Bioorg. Med. Chem. 15 (2007) 1212–1228.

Biochimica et Biophysica Acta 1820 (2012) 1886–1892

Contents lists available at SciVerse ScienceDirect

Biochimica et Biophysica Acta

journal homepage: www.elsevier.com/locate/bbagen

Different mechanisms of hepatitis C virus RNA polymerase activation by cyclophilin A and B in vitro

Leiyun Weng [a], Xiao Tian [a], Yayi Gao [a], Koichi Watashi [b], Kunitada Shimotohno [c], Takaji Wakita [b], Michinori Kohara [d], Tetsuya Toyoda [a,d,e,*]

[a] Unit of Viral Genome Regulation, Institut Pasteur of Shanghai, Chinese Academy of Sciences, 411 Hefei Road, 200025 Shanghai, People's Republic of China
[b] Department of Virology II, National Institute of Health, 1-23-1 Toyama, Shinjuku, Tokyo 132-8640, Japan
[c] Chiba Institute of Technology, 2-17-1 Tsudamuna, Narashino, Chiba 275-0016, Japan
[d] Department of Microbiology and Cell Biology, The Tokyo Metropolitan Institute of Medical Science, 2-1-6 Kamikitazawa, Setagaya-Ku, Tokyo 156-8506, Japan
[e] Choju Medical Institute, Fukushimura Hospital, 19-14 Azanakayama, Noyori-cho, Toyohashi, Aichi 441-8124, Japan

ARTICLE INFO

Article history:
Received 26 April 2012
Received in revised form 25 July 2012
Accepted 21 August 2012
Available online 28 August 2012

Keywords:
HCV
RNA polymerase
Cyclophilin A
Cyclophilin B

ABSTRACT

Background: Cyclophilins (CyPs) are cellular proteins that are essential to hepatitis C virus (HCV) replication. Since cyclosporine A was discovered to inhibit HCV infection, the CyP pathway contributing to HCV replication is a potential attractive stratagem for controlling HCV infection. Among them, CyPA is accepted to interact with HCV nonstructural protein (NS) 5A, although interaction of CyPB and NS5B, an RNA-dependent RNA polymerase (RdRp), was proposed first.
Methods: CyPA, CyPB, and HCV RdRp were expressed in bacteria and purified using combination column chromatography. HCV RdRp activity was analyzed in vitro with purified CyPA and CyPB.
Results: CyPA at a high concentration (50× higher than that of RdRp) but not at low concentration activated HCV RdRp. CyPB had an allosteric effect on genotype 1b RdRp activation. CyPB showed genotype specificity and activated genotype 1b and J6CF (2a) RdRps but not genotype 1a or JFH1 (2a) RdRps. CyPA activated RdRps of genotypes 1a, 1b, and 2a. CyPB may also support HCV genotype 1b replication within the infected cells, although its knockdown effect on HCV 1b replicon activity was controversial in earlier reports.
Conclusions: CyPA activated HCV RdRp at the early stages of transcription, including template RNA binding. CyPB also activated genotype 1b RdRp. However, their activation mechanisms are different.
General significance: These data suggest that both CyPA and CyPB are excellent targets for the treatment of HCV 1b, which shows the greatest resistance to interferon and ribavirin combination therapy.

1. Introduction

Hepatitis C virus (HCV[1]), which belongs to the *Flaviviridae* family, has a positive-strand RNA genome, and its replication is regulated by viral and cellular proteins [1]. The genome encodes a large precursor polyprotein that is cleaved by host and viral proteases to generate at least 10 functional viral proteins: core, envelope 1 (E1), E2, p7, nonstructural protein 2 (NS2), NS3, NS4A, NS4B, NS5A, and NS5B [2]. NS5B is an RNA-dependent RNA polymerase (RdRp) [3–5].

HCV frequently establishes a persistent infection that leads to chronic hepatitis, liver cirrhosis, and hepatocellular carcinoma [6,7]. More than 170 million individuals worldwide are infected with HCV [8], and the challenge of developing HCV treatment continues. First, combination therapy with pegylated interferon α (Peg-IFNα) and ribavirin led to a sustained virological response (SVR) in approximately 55% of patients infected with any HCV genotype and 42–46% of patients with genotype 1 [9,10]. However, many patients could not tolerate the serious adverse effects. Triple therapy consisting of an NS3/NS4A protease inhibitor (boceprevir or telaprevir), Peg-IFN (α-2a or α-2b), and ribavirin was then introduced, and it has become the standard regimen for genotype 1 infection. SVR improved significantly (from 63% to 75%), and the treatment duration decreased from 12 to 6 months [11,12]. However, triple therapy is more toxic than combination therapy [13].

Nonimmunosuppressant cyclosporine A (CsA) analogues/CyP inhibitors such as DEBIO-025 (Alisporivir) [14], NIM811 [15], and SCY-635 [16] are also the most expected candidates for use as anti-HCV drugs because their resistance selection is rare compared with other direct-acting antiviral agents, and the HCV resistant to

Abbreviations: BSA, bovine serum albumin; CsA, cyclosporine A; CyP, cyclophilin; DTT, dithiothreitol; E, envelope; EDTA, ethylenediaminetetraacetic acid; GST, glutathione S-transferase; HCV, hepatitis C virus; NS, nonstructural protein; PPI, peptidyl prolyl *cis/trans*-isomerases; Peg-IFN, pegylated interferon-α; PMSF, phenylmethanesulfonylfluoride; RT-PCR, reverse transcription polymerase chain reaction; RdRp, RNA-dependent RNA polymerase; SDS-PAGE, sodium dodecyl sulfate polyacrylamide gel electrophoresis analysis; SVR, sustained virological response; ΔPPI, PPI knockout; wt, wild type

* Corresponding author at: Choju Medical Institute, Fukushimura Hospital, 19-4 Azanakayama, Noyori-cho, Toyohashi, Aichi 441-8124, Japan. Tel.: +81 532 46 7511; fax: +81 532 46 8940.
E-mail address: toyoda_tetsuya@yahoo.co.jp (T. Toyoda).

0304-4165/$ – see front matter © 2012 Elsevier B.V. All rights reserved.
http://dx.doi.org/10.1016/j.bbagen.2012.08.017

CyP inhibitors acquired mutations that allowed for reduced dependence on CyPs [17,18].

CyP was originally discovered as a cellular factor with high affinity for CsA [19]. CyPs comprise a family of peptidyl prolyl *cis/trans*-isomerases (PPI) that catalyze the *cis–trans* interconversion of peptide bonds amino terminal to proline residues, facilitating protein conformation changes [20]. CyPs are potential antiviral targets because CyPA was found to play a critical role in human immunodeficiency virus-1 infection [21,22]. The role of human CyPs as cellular cofactors in HCV replication was first suggested upon discovery of the anti-HCV effect of CsA [23–26]. Although the completion of a binding assay and the mapping of resistance initially suggested that NS5B was a viral target for CsA [27–29], recent papers have pointed to CyPA and NS5A as the central virus–host interaction involved in HCV replication [30–36]. Despite this unfavorable evidence, we analyzed the effect of CyPA and CyPB on HCV RdRp of various genotypes in vitro and found differences in genotype specificity and the mechanism of HCV RdRp activation.

2. Materials and methods

2.1. Purification of HCV RdRp

HCV RNA RdRps with C-terminal 21 amino acid deletion of 1a (H77 and RMT), 1b (HCR6, NN, and Con1), and 2a (JFH1 and J6CF) were expressed in *E. coli* Rosetta/pLysS and purified as described previously [37–40]. The purified HCV RdRps (5 μM, >95% pure) were stocked in 20 mM Tris–HCl (pH 8.0), 500 mM NaCl, 1 mM ethylenediaminetetraacetic acid (EDTA), 5 mM dithiothreitol (DTT), 5% glycerol, and 1 mM phenylmethanesulfonylfluoride (PMSF) at −80 °C. The yield of HCV RdRps is approximately 1.7 mg from a 1-L bacterial culture. The purified HCV RdRps were as shown in Fig. S1 of Weng et al. [38]. The protein purities were determined by sodium dodecyl sulfate polyacrylamide gel electrophoresis analysis (SDS-PAGE), using ImageJ 1.46 (http://rsbweb.nih.gov/ij/).

2.2. Construction of CyP-expressing plasmids

Human CyPA and CyPB were cloned from total RNA extracted from 293T cells, using a reverse transcription-polymerase chain reaction (RT-PCR) kit (Takara, Dalian, China) as published previously [29]. After being digested with *Bam*HI and *Eco*RI, they were cloned into the same site of pGEX-6P-3 (GE Healthcare, Bucks, UK), resulting in pGEXCyPA and pGEXCyPB, respectively. CyPBΔPPI, the enzymatic inactive mutant of CyPB, was PCR cloned into pGEX-6P-3 from pCMV-CyPBΔPPIFL [29], resulting in pGEXCyPBΔPPI. CyPAΔPPI was produced by the introduction of the R55A and F60A mutations using a QuickChangeII Site-Directed Mutagenesis Kit (Stratagene, St. Clara, CA, USA) and primers (5′-GTTCCTGCTTTCACGCCATTATTCCAGGGG CCATGTGTCAGGGTG-3′ and 5′-CACCCTGACACATGGCCCCTGGAATAA TGGCGTGAAAGCAGGAAC-3′).

2.3. Purification of CyPs

E. coli Rosetta were transformed using pGEXCyPA, pGEXCyPAΔPPI, pGEXCyPB, and pGEXCyPBΔPPI. GST-tagged CyPA, CyPB, CyPAΔPPI, and CyPBΔPPI were induced with 1 mM isopropyl β-D-1-thiogalactopyranoside at 18 °C for 4 h. The bacteria were harvested and stocked at −20 °C. After thawing on ice, the bacteria were lysed in 4 packed cell volumes of phosphate-buffered saline, 0.1% Triton X-100, 1 mM EDTA, 1 mM DTT, and 1 mM PMSF. After being clarified by centrifugation at 10,000×*g* for 30 min at 4 °C and filtered through a 0.45-μm nitrocellulose filter, the extract was incubated with Glutathione Sepharose 4B (GE Healthcare) for 30 min at 4 °C. After the resin was washed with 50 mM Tris–HCl (pH 8.0), 500 mM NaCl, 1 mM EDTA, 1 mM DTT, and 1 mM PMSF, the GST-CyP was eluted using 50 mM Tris–HCl (pH 8.0), 500 mM NaCl, 1 mM EDTA, 1 mM DTT, 10 mM reduced glutathione, and 1 mM PMSF, followed by gel filtration through a Superdex 200 column (GE Healthcare) in 20 mM Tris–HCl (pH 8.0), 500 mM NaCl, 1 mM EDTA, 1 mM DTT, and 10% glycerol. The eluted GST-CyP were diluted to 50 mM NaCl and applied to a MonoQ (GE Healthcare) in 20 mM Tris–HCl (pH 9.0), 50 mM NaCl, 1 mM EDTA, 1 mM DTT, and 10% glycerol. GST-CyPB and GST-CyPBΔPPI were chromatographed using a continuous NaCl gradient of 50–1000 mM. The purified CyPs were stocked at −20 °C.

2.4. In vitro HCV transcription with CyPs

In vitro HCV transcription with CyPs was done as previously described [37–40]. Briefly, the indicated amounts of the CyPs were incubated in 50 mM Tris–HCl (pH 7.5), 200 mM monopotassium glutamate, 3.5 mM $MnCl_2$, 1 mM DTT, 0.5 mM GTP, 200 nM of a 184-nt in vitro transcribed model RNA template (SL12-1S), 100 U/mL of human placental RNase inhibitor, and 100 nM HCV RdRp at 29 °C for 30 min. After preincubation, RdRp was incubated for an additional 90 min with 50 μM ATP, 50 μM CTP, or 5 μM [α-^{32}P]UTP. The RNA products were analyzed using 6% PAGE containing 8 M urea after being purified by phenol/chloroform extraction and ethanol precipitation. The amount of RNA products was analyzed using Typhoon Trio (GE Healthcare).

2.5. RNA filter-binding assay with CyPA and CyPB

An RNA filter-binding assay with CyPA and CyPB was performed as previously described [37,38,40]. Briefly, [^{32}P]-SL12-1S was incubated in 25 μL of 50 mM Tris–HCl (pH 7.5), 200 mM monopotassium glutamate, 3.5 mM $MnCl_2$, 1 mM DTT, and 5 pmol of HCV RdRp with 375 pmol (75×) of CyPA and 25 pmol (5×) of CyPB at 29 °C for 30 min.

2.6. Chemicals and radioisotopes

[α-^{32}P]UTP (800 Ci/mmol, 40 mCi/mL) was purchased from PerkinElmer Life Sciences (Waltham, MA, USA). The nucleotides were purchased from GE Healthcare. The human placental RNase inhibitor T7 RNA polymerase and PrimeSTAR HS DNA polymerase were purchased from Takara. The bacteria were purchased from Novagen (Merck Chemicals, Darmstadt, Germany).

2.7. Statistical analysis

The statistical data were evaluated using Student's *t* test, with $p<0.05$ indicating statistical significance.

3. Results

3.1. Purification of CyPA and B

First, glutathione S-transferase (GST)-tagged CyPA, CyPB, the PPI inactive CyPA (CyPAΔPPI), and CyPB (CyPBΔPPI) were purified using Glutathione Sepharose 4B affinity chromatography. CyPA and CyPAΔPPI were further purified through a Superdex 200 column (Fig. S1). After the Superdex 200 gel filtration, to remove the contaminating nucleic acids, CyPB and CyPBΔPPI were further purified through MonoQ anion exchange chromatography by a continuous NaCl gradient of 50–1000 mM because CyPB has a strong affinity for nucleic acids. Each was eluted with 210–385 mM NaCl (Fig. S2). The purification scheme and purified CyPs are shown in Fig. 1. The yields of CyPA and CyPAΔPPI were approximately 3 mg from a 1-L bacterial culture. CyPA and CyPAΔPPI were >95% pure and stocked at 5 mg/mL in 20 mM Tris–HCl (pH 8.0), 500 mM NaCl, 1 mM EDTA, 1 mM DTT, and 10% glycerol. CyPB and CyPBΔPPI were stocked at 5 mg/mL in 20 mM Tris–HCl (pH 9.0), 500 mM NaCl, 1 mM EDTA, 1 mM DTT,

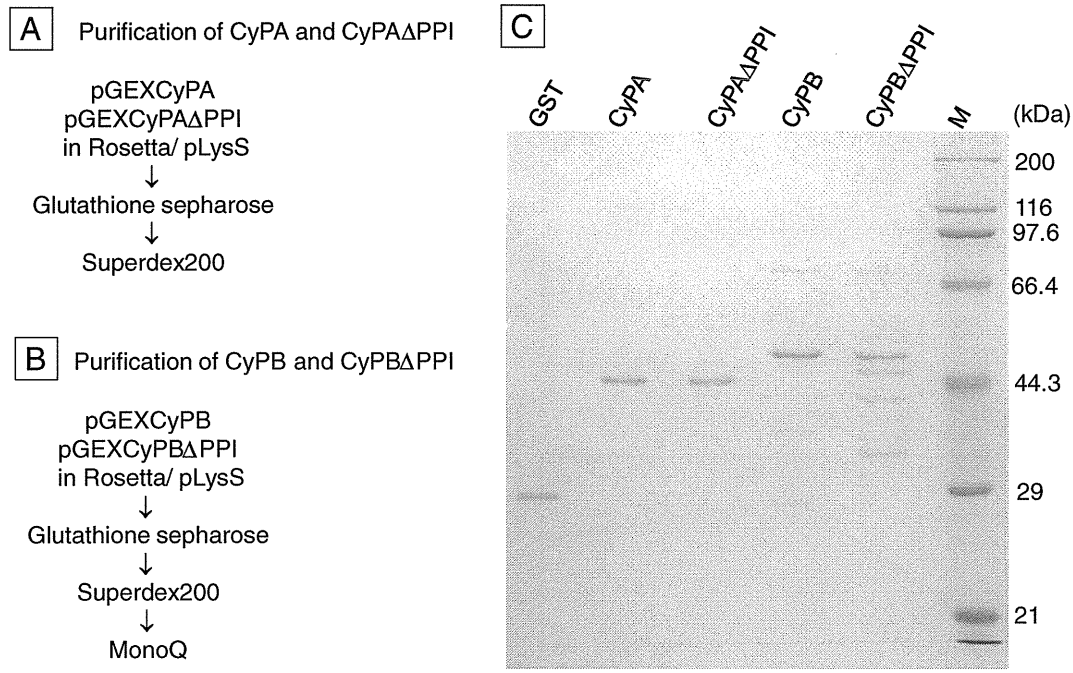

Fig. 1. Cyclophilin purification. The purification schemes of cyclophilin A (CyPA) and the peptidyl prolyl isomerase-inactive mutant protein of CyPA (CyPAΔPPI) (A), cyclophilin B (CyPB) and CyPBΔPPI (B), and sodium dodecyl sulfate-polyacrylamide gel electrophoresis (SDS-PAGE) (C) with 5 pmol each of purified glutathione S-transferase (GST; 28.3 kDa), GST-CyPA (44.9 kDa), GST-CyPAΔPPI (44.7 kDa), GST-CyPB (52.1 kDa), and GST-CyPBΔPPI (52 kDa) were separated through 10% SDS-PAGE and stained with Coomassie brilliant blue. The sizes of the molecular weight standards (M) are indicated on the right side of the gel. Their final elution profiles are shown in Figs. S1 and S2.

and 10% glycerol. The yields of CyPB and CyPBΔPPI were approximately 1 mg from a 1-L bacterial culture. The purities of CyPB and CyPBΔPPI were >95% and >90%, respectively.

3.2. HCV 1b and JFH1 (2a) transcription in vitro with CyPA and CyPB

The dose–response effects of CyPA and CyPB were examined using an in vitro transcription system of HCR6 (1b) and JFH1 (2a) RdRp wild type (wt). CyPA and CyPB were added to the optimal HCV in vitro transcription condition while the RNA synthesis was in the log phase [4,37]. RdRp (100 nM) was incubated with 0, 50 (ratio to RdRp: 0.5×), 100 (1×), 200 (2×), 500 (5×), and 1000 nM (10×) CyPA and CyPB, GST, or bovine serum albumin (BSA) in GTP (the initiating nucleotide) and an RNA template for 30 min, followed by elongation with ATP, CTP, and UTP for 90 min. CyPA enhancement was further tested using 2 (20×), 5 (50×), 7.5 (75×), and 10 (100×) μM because the enhancement effect of CyPA under 1 μM (10×) was unclear. Fig. S3 shows the autoradiography of HCV HCR6 (1b) and JFH1 (2a) RdRpwt with CyPA and CyPB, the graphs of which were drawn using the data from 3 independent experiments (Fig. 2).

The CyPA activation of both RdRps showed 2 reaction speeds. The first-order ratio of CyPA to HCR6 (1b) RdRpwt<50× is fitted as a linear regression curve, the equation for which is $y=0.07x$ (CyPA-to-RdRp ratio) + 0.7. The linear regression curve fitting of the ratio >50× is $y=0.4x$ (CyPA-to-RdRp ratio) − 17 when calculated from 3 points. That of CyPA to JFH1 (2a) RdRpwt is fitted to a similar linear regression, $y=0.09x$ (CyPA-to-RdRp ratio) + 0.9 (the CyPA-to-RdRp ratio<50×). HCVR6 (1b) and JFH1 (2a) RdRps were activated by 100× CyPA to 25-±0.2- and 19-±1-fold, respectively.

The CyPB activation of HCR6 (1b) RdRpwt occurred in a dose-dependent manner and fitted a sigmoid curve, and the enhancement effect reached a plateau (9.4×) at the ratio of 5×. Neither GST nor BSA enhanced HCR6 (1b) RdRpwt. CyPB, GST, and BSA did not enhance JFH1 (2a) RdRpwt (<1.5×) at the concentrations described earlier.

3.3. Effect of the PPI inactive mutant proteins of CyPA and CyPB

CyP has PPI activity. To test the contribution of PPI activity to HCV HCR6 (1b) and JFH1 (2a) RdRpwt activation, the activation effect of the PPI inactive mutant proteins, CyPAΔPPI at 100× (10 μM) and CyPBΔPPI at 2× (200 nM), were tested together with 100× (10 μM) GST and BSA (Fig. 3). CyPA enhanced JFH1 (2a) RdRpwt 17.6×, whereas CyPAΔPPI enhanced it 16.2×. This difference is statistically significant (Student's t test, $p<0.05$). CyPA enhanced HCR6 (1b) RdRpwt activity 27.7×, whereas CyPAΔPPI enhanced it 16.0×. BSA slightly inhibited both RdRps at the same concentration in this experiment. As shown in Fig. 2C and D, it can be concluded that BSA has no effect on HCV transcription. GST enhanced JFH1 (2a) RdRpwt activity 5.0×, but it did not affect HCR6 (1b) RdRpwt activity. CyPB enhanced HCR6 (1b) RdRpwt activity 2.3×, whereas CyPBΔPPI enhanced it 1.7×. This difference is also statistically significant (Student's t test, $p<0.05$). JFH1 (2a) RdRpwt was not activated by CyPB or CyPBΔPPI.

3.4. CyP activation steps of HCV transcription

The HCV transcription steps of CyP enhancement were analyzed by the sequential addition of CyPs during in vitro transcription (Fig. 4). CyPA enhanced HCR6 (1b) and JFH1 (2a) RdRpwt, whereas CyPB enhanced HCR6 (1b) RdRpwt when HCV RdRps were incubated with them from the start of transcription (initiation). The CyP effect was then tested after their addition during the elongation period after HCV RdRps was initiated with GTP. CyPA (100×; 10 μM) and CyPB (5×; 500 nM) were added to HCV RdRps after the 30-min incubation with GTP, when 3 GTPs were incorporated at the 5′ end of the products. CyPB did not enhance HCR6 (1b) or JFH1 (2a) RdRp when added during the elongation period, although it enhanced HCV RdRp when added at the start of transcription. CyPA enhanced HCR6 (1b) and JFH1 (2a) RdRp activity only 1.6× (Student's t test, $p<0.05$) and 2.1× ($p<0.01$), respectively, when added during the elongation step. These results suggest that CyPA and CyPB activated only the transcription initiation step of HCV RdRps.

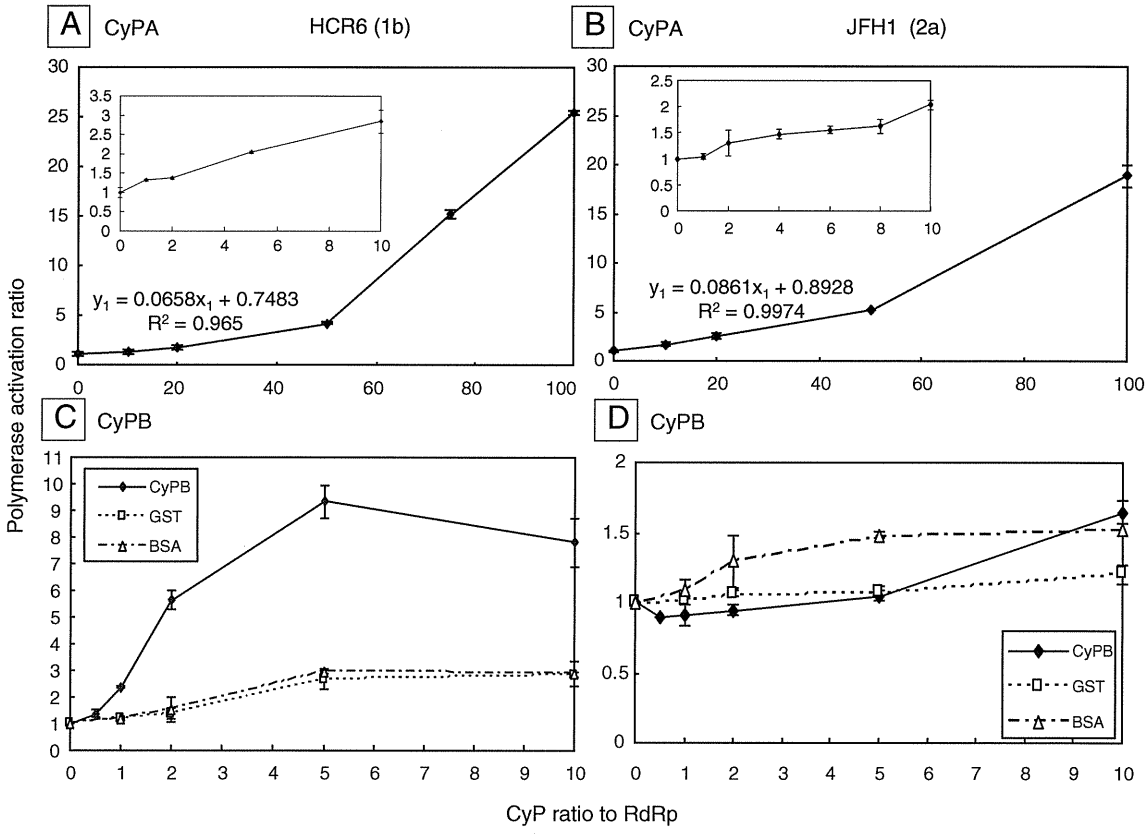

Fig. 2. Dose–response curve of cyclophilin A (CyPA) and cyclophilin B (CyPB) in hepatitis C virus (HCV) transcription in vitro. The dose–response curve of the HCV RdRp activation of CyPA in HCR6 (1b) RdRpwt (A) and JFH1 (2a) RdRpwt (B) CyPB in HCR6 (1b) RdRpwt (C) and JFH1 (2a) RdRpwt was drawn from the image analysis of Fig. S3. Insets A and B indicate that of 0, 0.5×, 1×, 2×, 5×, and 10× of CyPA to RdRp. The first-order ratio of the curves of A and B were fit by linear regression, and the calculated equations are indicated in the graph. The mean relative polymerase activation ratio and standard deviation (error bar) were calculated from 3 independent measurements.

The effects of 75× CyPA and 5× CyPB on the RNA-binding activity of HCR6 (1b) and JFH1 (2a) RdRp were then tested (Fig. 4E). The effects of HCR6 (1b) and JFH1 (2a) RdRp with CyPA were 10.1-±0.56- and 6.6-±0.68-fold of that without CyPA, respectively. The effect of HCR6 (1b) RdRp with CyPB was 3.1-±0.3-fold of that without CyPB. The RNA-binding activity of HCV RdRps was thus enhanced by the addition of CyPA and CyPB.

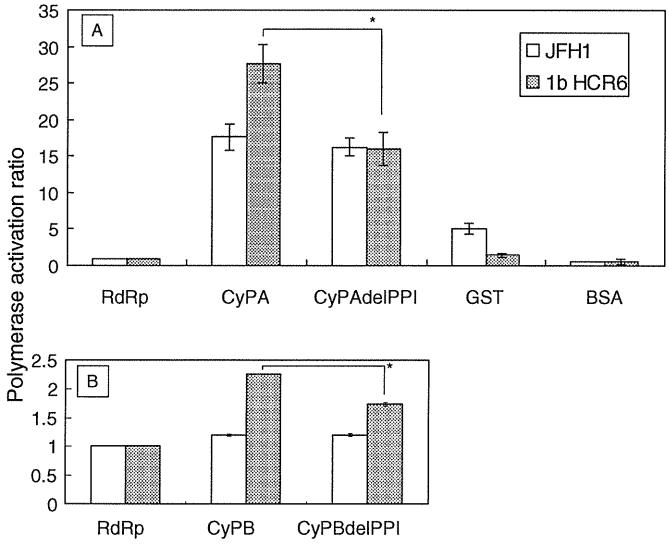

Fig. 3. Effects of cyclophilin A (CyPA) and cyclophilin B (CyPB) with and without peptidyl prolyl isomerases activity on hepatitis C virus (HCV) JFH1 (2a) and HCR6 (1b) RdRp. HCV HCR6 (1b) and JFH1 (2a) RdRpwt (100 nM) were incubated with 100× (10 μM) of CyPA, CyPAΔPPI, glutathione S-transferase (GST), and bovine serum albumin (BSA) (A). HCV RdRps were incubated with 5× (500 nM) of CyPB, CyPBΔPPI, GST, and BSA (B). The mean relative polymerase activity and standard deviation (error bar) were calculated from 3 independent measurements. *p<0.01 (Student's *t* test).

3.5. Effect of CyP activation on RdRp of various HCV genotypes

The CsA sensitivity differed among the HCV genotypes [41]. Therefore, we tested the effects of CyPA and CyPB activation on NN (1b), H77 (1a), RMT (1a), and J6CF (2a) RdRp (Fig. 5). RdRp activity was compared with and without 50× (5 μM) CyPA and 5× (500 nM) CyPB. At their respective concentrations, CyPA activated all of the tested HCV RdRps by 3.9–5.3×, but CyPB activated only 1b RdRps (8–10×). CyPB slightly activated J6CF (2a) RdRp (approximately 4×), but it did not activate the 1a or JFH1 (2a) RdRps (1.4–1.8×).

4. Discussion

Since CsA was discovered to inhibit HCV infection [23–26], the CyP pathway contributing to HCV replication has been proposed as a potential stratagem for controlling HCV infection. Reports about the roles of CyPA in HCV replication via NS5A have been accumulating [33–35,42–44]. However, the effect of CyP inhibitors varied on the RNA-binding activity of NS5B [41,45], and DEBIO-025 decreased CyPB levels in patients [46]. Controversial results of CyPA and CyPB knockout experiments on HCV replicon activity were reported [29,30,47]. Therefore, the effects of CyPA and CyPB on HCV RdRp were carefully analyzed again in vitro.

In this study, we demonstrated that CyPA and CyPB activated HCV 1b RdRp in vitro by completely different kinetics using purified CyPs

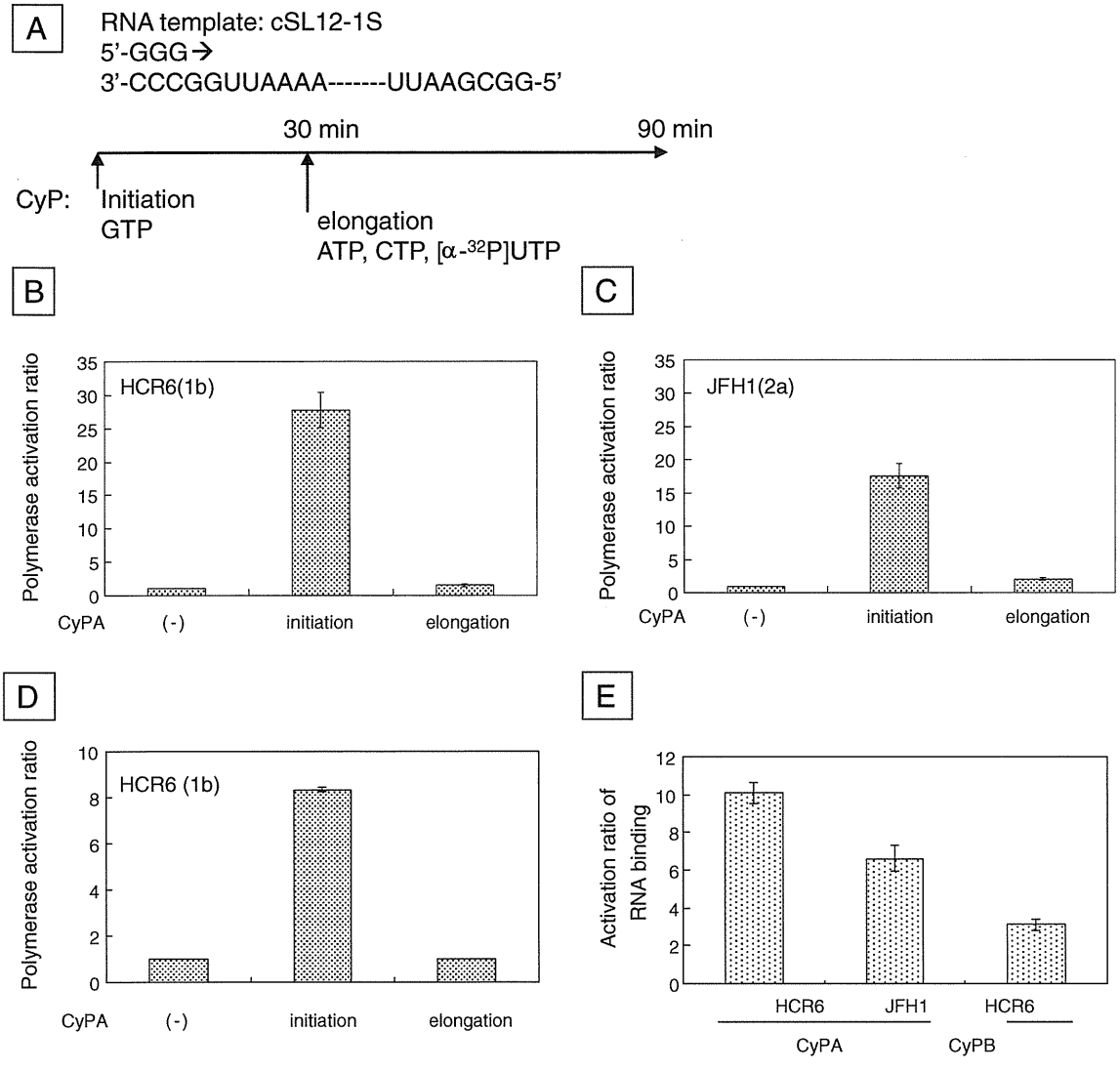

Fig. 4. Hepatitis C virus (HCV) RdRp activation effects of cyclophilin A (CyPA) and cyclophilin B (CyPB) on transcription initiation and elongation. The polymerase activation effect of the timing of the CyPA or CyPB addition was examined. The sequence of the model RNA template (SL12-1S) and experimental design are shown in A. CyPA 100× (10 μM) was incubated with HCR6 (1b) RdRpwt (A) and JFH1 (2a) (B) RdRp during preincubation with 0.5 mM GTP (initiation) or after preincubation (elongation). CyPB 5× (500 nM) was incubated with HCVR6 (1b) RdRpwt during preincubation with 0.5 mM GTP (initiation) or after the preincubation (elongation) (C). The mean relative polymerase activation ratio and standard deviation (error bar) were calculated from 3 independent measurements. The effect of the 100× CyPA and 5× CyPB on RNA template binding was examined (E).

and HCV RdRps (Fig. 2), which indicated that the mechanism of their HCV RdRp activation differed despite their similar structures [48–50]. Kinetic analysis of CyPA on HCR6 (1b) and JFH1 (2a) RdRp indicated that it had a similar activation mechanism on both HCV RdRps. CyPA did not activate HCV RdRp at low concentrations, but it did activate it at >50× molar excess to it. The unusual dose of CyPA activating HCV RdRp (Fig. 2) postulates that HCV RdRp may be surrounded by CyPA in vitro and factors involving CyPA and HCV RdRp interaction, such as NS5A, in the HCV replication complex of the infected cells [27,28,31,36,51–53] because the interaction of CyPA and HCV RdRp was weak (Fig. S4).

Although some controversial results were obtained from those of Heck et al. [54], the studies agree that CyPB also activated HCV 1b RdRp in vitro. The activation kinetics of CyPB on HCR6 (1b) RdRp showed a sigmoid-like curve (Fig. 2) that suggested an allosteric effect of CyPB on RdRp activity. CyPB may interact with HCV RdRp as a cofactor and directly activate HCR6 (1b) RdRp. The HCV RdRp–CyPB complex was likely to interact more with CyPB, and its activation plateaued at the CyPB/RdRp ratio of 5:1 (Fig. 2C). The CyPB activation curves of Heck et al. [54] also plateaued. These data from the 2 independent groups support the weak interaction between CyPB and HCV 1b RdRp (Fig. S4).

CyPA did not show genotype specificity in the current study (Fig. 5A), a finding that agrees with those of CyPA knockdown, DEBIO-025, and CsA experiments [30,43,55]. CyPB activation showed genotype specificity (Fig. 5B) [54]; CyPB activated 1b and J6CF (2a) RdRp but did not activate 1a or JFH1 (2a) RdRp. Both reports agreed with the finding that JFH1 (2a) subgenomic replicon was independent of CyPB [41]. Although mutations accumulated in the NS5A region of CsA- or DEBIO-025-resistant HCV replicons, some mutations were found in the NS5B region [18,27,28,33,45].

Another controversial result between that of Heck et al. [54] and ours is the Mg^{2+}-dependency of the CyPB activation. The Mg^{2+} concentration in cells is 14–20 mM, and Mg^{2+} ions are distributed almost equally throughout the nuclei, mitochondria, and cytosol/endoplasmic reticulum [56]. The Mn^{2+} concentration in cells varies from report to report [57,58]. The optimal Mn^{2+} and Mg^{2+} concentrations in the HCV in vitro transcription used in this study were